الجمهورية الجزائرية الديمقراطية الشعبية

وزارة التعليم العالي والبحث العلمي

جامعة محمد البشير الإبراهيمي - برج بوعريريج

**People's Democratic Republic of Algeria**

**Ministry of Higher Education and Scientific Research**

**Mohamed El-Bachir El-Ibrahimi University – Bordj Bou Arreridj**

**Faculty of Science and Technology**

**Department of Electronics**

**Thesis**

Presented for the award of the MASTER's degree

**In**: Telecommunication

**Speciality**: Telecommunications System

**By**: Azzi, Ibnsina Faiz

**Subject**

# Applications of Metasurface Structures on Antenna Design for 5G Communications

Publicly defended on 30/06/ 2025, before the jury composed of:

| | | | |
|---|---|---|---|
| Mr.TITOUNI Salem | Grade | **MCB** | President |
| Mr.BELAZZOUG Massinissa | Grade | **MCB** | Examiner |
| Mr.MESSAOUDENE Idris | Grade | **MCA** | Supervisor |

Academic Year 2024/2025

# Acknowledgment:

At the outset of this thesis, I would like to thank Allah, the Almighty, for granting me the opportunity to reach this stage of knowledge, and for bestowing upon me the strength, courage, and patience to complete this humble work.

I express my sincere gratitude to my supervisor, Mr. Idris MESSAOUDENE, for his invaluable guidance, continuous support, and unwavering patience throughout this project. His insightful advice and constant encouragement greatly motivated me and played a key role in the successful completion of this work. I hope this thesis stands as a modest reflection of my deep appreciation for his dedication and exemplary mentorship.

I am also deeply thankful to the esteemed jury members for dedicating their time to evaluate my research. Their valuable remarks and constructive feedback have not only enriched the quality of this work but will also serve as a guide for my future academic and professional endeavors.

My heartfelt thanks go as well to all the professors who have accompanied me throughout my academic journey. Their dedication to teaching, passion for their fields, and willingness to share their knowledge have significantly contributed to my personal and intellectual growth.

Lastly, I extend my gratitude to everyone who, in any way, supported or inspired me during the preparation of this thesis. Their contributions, though sometimes unseen, are sincerely appreciated.

# Dedications

I dedicate this modest work to:

My beloved parents, whose unwavering love, patience, and sacrifices have laid the foundation for every success I have achieved. Their enduring belief in my potential has been a constant source of strength and motivation throughout my academic journey.

To my dear sisters **Asla**, **Isra**, and **Sondosse**, for their constant support and encouragement.
To my youngest sister **Taiba**, with heartfelt wishes for success in her upcoming baccalaureate exams.
To my brother **Nawfel**, who generously loaned me his computer and stood by me when I needed it most.
To my youngest brother **Baraa**, whose presence fills our home with energy and joy.

To my sister **Asla** and her husband **Nassim**, for their continuous encouragement and support.
To their child, **Fares Faraisso**, who made me laugh, drove me crazy, and brought moments of joy to this journey .

To my amazing friends **Yassin**, **Yasser**, **Lyna**, **Youcera**, and **Lakher** — with special thanks to **Lyna** and **Youcera** for their valuable help during the preparation of this thesis, and to **Yassin**, whose encouragement carried me through my entire university journey.

And finally, to all the other friends whose names I haven't mentioned, but who supported me with their words, presence, and kindness — this work is also dedicated to you.

.

# Abstract

This comprehensive study explores two significant concepts in modern electromagnetics: Metasurfaces (MTS) and Characteristic Mode Analysis (CMA). Metasurfaces represent two-dimensional metamaterial structures that enable unprecedented control over electromagnetic waves through subwavelength elements arranged in planar configurations. Characteristic Mode Analysis provides a powerful mathematical framework for understanding the inherent resonance behavior of conducting bodies, offering valuable insights for antenna design and optimization. This document details the theoretical foundations, various types, analytical methodologies, and practical applications of both technologies. The synergistic relationship between MTS and CMA is highlighted, particularly in advanced antenna design, telecommunications, and emerging electromagnetic applications. By examining these complementary fields together, this work provides a holistic perspective on cutting-edge approaches to controlling and optimizing electromagnetic wave propagation and radiation.



# Resumé

Cette étude approfondie explore deux concepts majeurs dans l'électromagnétisme moderne : les **métasurfaces (MTS)** et l'**analyse modale caractéristique (CMA)**. Les métasurfaces sont des structures métamatériaux bidimensionnelles permettant un contrôle sans précédent des ondes électromagnétiques grâce à des éléments sub-longueur d'onde disposés en configurations planes. L'analyse modale caractéristique offre un cadre mathématique puissant pour comprendre le comportement résonant intrinsèque des corps conducteurs, fournissant ainsi des informations précieuses pour la conception et l'optimisation des antennes. Ce document présente les fondements théoriques, les différentes classifications, les méthodologies d'analyse, ainsi que les applications pratiques des deux technologies. La synergie entre les MTS et la CMA est particulièrement mise en valeur, notamment dans la conception avancée d'antennes, les télécommunications et les applications électromagnétiques émergentes. En examinant ces domaines complémentaires, ce travail offre une perspective globale sur les approches de pointe permettant de contrôler et d'optimiser la propagation et le rayonnement des ondes électromagnétiques.

# ملخص

تهدف هذه الدراسة إلى تقديم تحليل منهجي لمفهومين محوريين في مجال الكهرومغناطيسية الحديثة، وهما: السطوح الفوقية (Metasurfaces - MTS) وتحليل الأنماط المميزة (Characteristic Mode Analysis - CMA). تُعد السطوح الفوقية بنى اصطناعية ثنائية الأبعاد تتميز بقدرتها على التحكم الدقيق في خصائص الموجات الكهرومغناطيسية، من خلال تصميم وحدات خلوية ذات أبعاد دون الطول الموجي، تُنظم بطريقة تُمكّن من ضبط الطور، والسعة، واستقطاب الموجة. في المقابل، يوفر تحليل الأنماط المميزة إطاراً رياضياً فعالاً لتحليل الأداء الكهرومغناطيسي للهياكل الموصلة، من خلال استخلاص الأنماط الرنينية الطبيعية، الأمر الذي يُسهم في تحسين تصميم الهوائيات وتوجيه الإشعاع بطريقة مثلى.تُعنى هذه الدراسة باستعراض الخلفيات النظرية، وتصنيفات البنى، والأساليب التحليلية المتعلقة بكل من MTS وCMA، مع التركيز على التطبيقات العملية في مجال تصميم الهوائيات المتقدمة. كما تسلّط الضوء على التكامل البنيوي والتحليلي بين هاتين التقنيتين، ومدى مساهمتهما في تطوير هوائيات عالية الكفاءة تلبي متطلبات أنظمة الاتصالات اللاسلكية الحديثة، لا سيما شبكات الجيل الخامس (G5). ومن خلال هذا التكامل، تُقدم الدراسة منظوراً علمياً متقدماً نحو تعزيز أداء الأنظمة الكهرومغناطيسية وتوسيع قدراتها الوظيفية.

# Table of Contents

# Table of Figures

# Liste of Table

# Acronym List

| Acronym | Full Form |
|---|---|
| **MTS** | Metasurfaces |
| **CMA** | Characteristic Mode Analysis |
| **$S_{11}$** | Reflection Coefficient Parameter (Return Loss) |
| **IRS** | Intelligent Reflecting Surfaces |
| **MIMO** | Multiple-Input Multiple-Output |
| **EFIE** | Electric Field Integral Equation |
| **MoM** | Method of Moments |
| **RWG** | Rao-Wilton-Glisson (basis functions) |
| **IRAM** | Implicitly Restarted Arnoldi Method |
| **CFIE** | Combined Field Integral Equation |
| **FMM** | Fast Multipole Method |
| **MLFMA** | Multi-Level Fast Multipole Algorithm |
| **ACA** | Adaptive Cross Approximation |
| **POD** | Proper Orthogonal Decomposition |
| **GPU** | Graphics Processing Unit |
| **MS** | Modal Significance |
| **Q** | Quality Factor (in resonance analysis) |
| **DRAs** | Dielectric Resonator Antennas |
| **RCS** | Radar Cross Section |
| **IoT** | Internet of Things |
| **dB(A/m)** | Decibel per Ampere per meter (used for surface current magnitude) |
| **GHz** | Gigahertz |
| **dBi** | Decibels relative to isotropic radiator (used for gain) |
| **SLL** | Side Lobe Level |
| **$\lambda_0$** | Free-space wavelength |

# General Introduction

The electromagnetic spectrum represents one of humanity's most valuable natural resources, enabling countless technologies from wireless communications to medical imaging. As demands on this limited resource grow exponentially with the advancement of wireless technologies, researchers continually seek new methods to manipulate, control, and optimize electromagnetic wave propagation and radiation. Two particularly promising approaches that have emerged in recent decades are Metasurfaces (MTS) and Characteristic Mode Analysis (CMA).

Metasurfaces are ultrathin metamaterial structures, typically composed of subwavelength elements arranged in a planar configuration. These structures can manipulate electromagnetic waves in ways that conventional materials cannot, enabling unprecedented control over wave properties such as phase, amplitude, polarization, and directionality. Unlike their three-dimensional metamaterial counterparts, metasurfaces offer advantages of reduced profile, lower loss, and easier fabrication, making them highly attractive for practical applications.

Characteristic Mode Analysis, on the other hand, provides a powerful mathematical framework for understanding the inherent resonance behavior of conducting bodies. By decomposing complex electromagnetic interactions into orthogonal modes with physical significance, CMA offers insights that traditional analytical approaches often obscure. This modal decomposition facilitates antenna design by revealing the fundamental radiation mechanisms of arbitrary structures.

The convergence of these two fields has opened new avenues for electromagnetic engineering. Metasurfaces designed with insights from CMA can achieve enhanced performance and functionality, while CMA applied to metasurface structures can reveal design principles that might otherwise remain hidden. Together, these technologies are driving innovations in telecommunications, sensing, imaging, and numerous other applications.

This thesis is structured into two main chapters. The **first chapter** presents a comprehensive theoretical study of **Metasurfaces (MTS)** and **Characteristic Mode Analysis (CMA)**. It outlines the fundamental principles, classifications, methodologies, and a wide range of

applications of both technologies, highlighting their potential in modern antenna design. The **second chapter** focuses on the **numerical results and discussion**, where two metasurface-based antenna designs are investigated. Detailed simulations and analyses are provided, comparing antenna performance with and without metasurface integration using CMA. The chapter includes return loss, gain, radiation patterns, and modal significance studies to demonstrate the effectiveness of metasurfaces guided by modal analysis. The thesis concludes with a general summary of findings and suggestions for future research directions.

# Chapter I: Theoretical Study

## I.1 Introduction

This comprehensive study aims to explore both metasurfaces and characteristic mode analysis in depth, examining their theoretical foundations, various types, analytical methodologies, and practical applications. By considering these complementary fields together, we provide a holistic perspective on cutting-edge approaches to controlling and optimizing electromagnetic wave propagation and radiation, with particular emphasis on applications in modern telecommunications and antenna design.

## I.2 Metasurfaces (MTS)

Metasurfaces are defined as two-dimensional arrays of subwavelength elements (meta-atoms) designed to manipulate electromagnetic waves in ways that conventional materials cannot. These planar structures represent the two-dimensional counterparts of three-dimensional metamaterials, offering similar exotic electromagnetic properties while maintaining a significantly reduced profile, as illustrated in Figure 1. According to Bukhari et al [1], metasurfaces can be characterized as "planar metamaterials" where "the thickness and periodicity of the individual elements (scatterers) are small in comparison to the wavelength of operation."

From a physical perspective, metasurfaces can be understood through the Huygens principle, which states that each point on a wavefront act as a secondary source. When an electromagnetic wave interacts with a metasurface, it induces electric and magnetic dipole moments in the meta-atoms, which then re-radiate to form a modified wavefront. According to Schelkunoff's principle, these induced currents are equivalent to tangential electric and magnetic fields that control the electromagnetic response of the surface [1].

A fundamental characteristic that distinguishes metasurfaces from traditional frequency selective surfaces (FSS) is the subwavelength nature of their constituent elements. While FSS typically have periodicities on the order of half the operational wavelength ($\lambda/2$), metasurfaces employ much smaller elements, allowing them to be treated as homogeneous structures characterized by effective parameters. This homogenization allows for powerful analytical approaches based on generalized sheet transition conditions using electric and magnetic surface

susceptibilities [2].

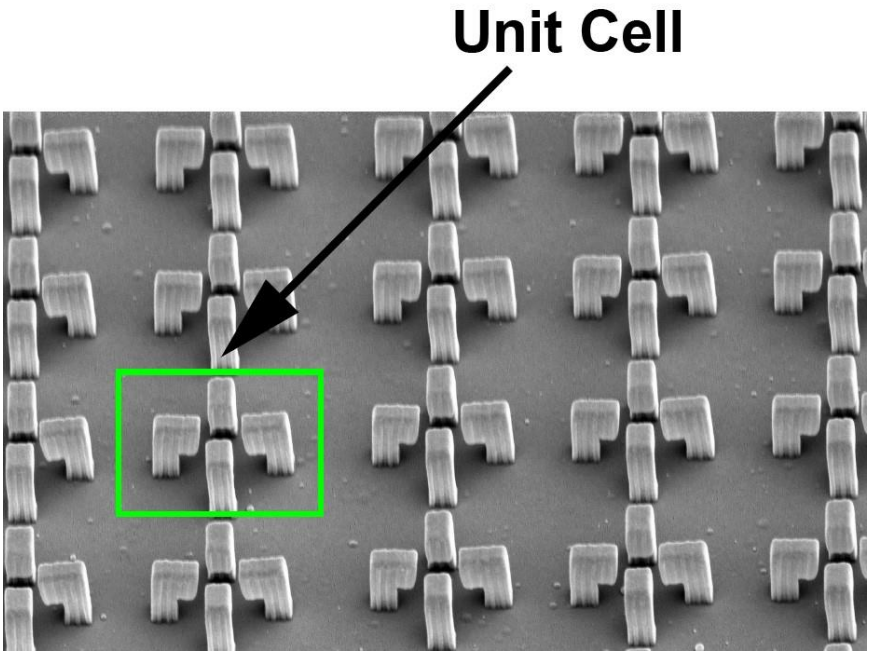


Figure 1:Basic structure of a metasurface

One of the most significant phenomena associated with metasurfaces is the phase discontinuity or phase jump that occurs when an electromagnetic wave passes through the structure. This discontinuity leads to

a generalized law of refraction and reflection that extends Snell's law, as formulated by Yu et al. [3]:

$$n1sin(\theta i) - n2sin(\theta t) = \left(\frac{\lambda 0}{2\pi}\right)\left(\frac{d\Phi}{dx}\right) \#(1)$$

where $n_1$ and $n_2$ are the refractive indices of the incident and transmission media, $\theta_i$ and $\theta_t$ are the angles of incidence and transmission, $\lambda_0$ is the free-space wavelength, and $d\Phi/dx$ is the phase gradient along the metasurface. This equation demonstrates how metasurfaces can achieve anomalous reflection and refraction effects that are impossible with conventional materials.

The ability of metasurfaces to tailor both electric and magnetic field components of electromagnetic waves allows them to overcome limitations of traditional surfaces. Particularly noteworthy are Huygens metasurfaces, which can be designed to have negligible reflection losses by carefully balancing electric and magnetic polarizabilities [4].

### I.2.1 Types of MTS

Metasurfaces can be classified according to various criteria, including their operational

mechanisms, structural characteristics, functionality, and tunability. Understanding these different types provides insight into the diverse applications and design approaches in this rapidly evolving field.

- **Classification Based on Operational Mechanism**

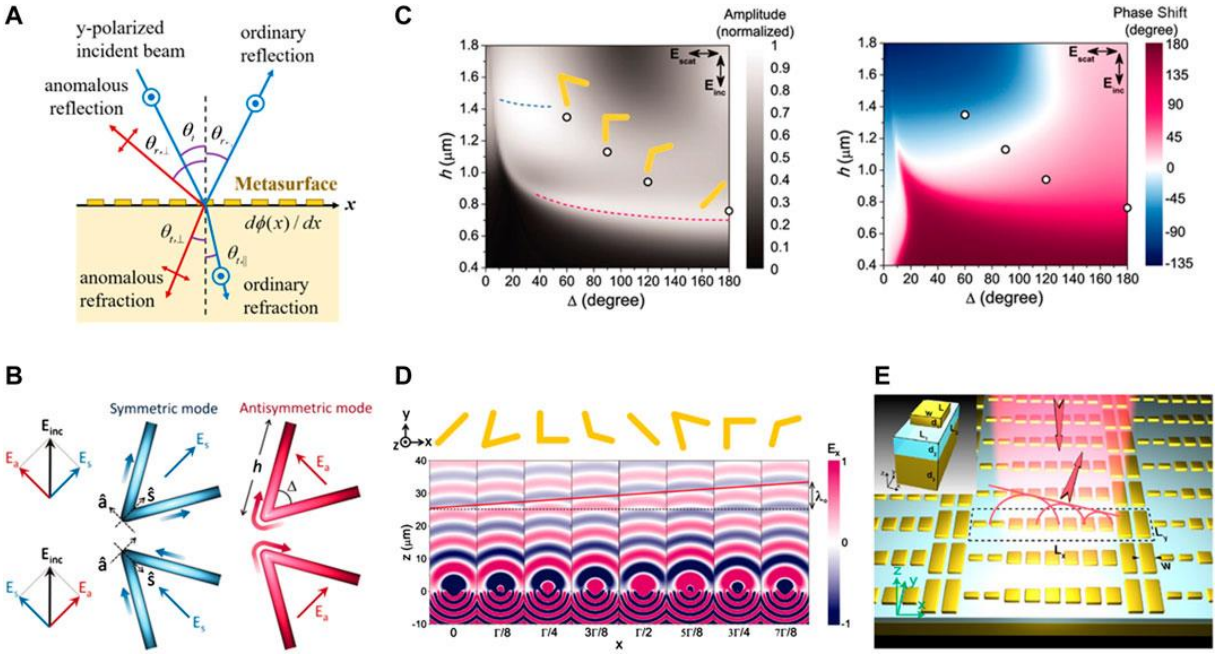


Figure 2:Various types of metasurfaces: (A) Schematic of generalized Snell's law metasurface, (B) Plasmonic metasurface, (C) Dielectric metasurface, and (D) Hybrid metasurface combining plasmonic and dielectric elements, (E) electric field *[5]*

**Plasmonic Metasurfaces:** These metasurfaces utilize metallic nanostructures that support surface plasmon resonances—collective oscillations of free electrons at metal-dielectric interfaces. Plasmonic metasurfaces can achieve strong field enhancement and confinement but typically suffer from ohmic losses, especially at optical frequencies [6].

**Dielectric Metasurfaces:** Composed of high-index dielectric resonators, these metasurfaces leverage Mie resonances rather than plasmonic effects. They typically exhibit lower losses than their metallic counterparts, making them particularly attractive for optical applications that require high efficiency [7].

**Hybrid Metasurfaces:** These combine both metallic and dielectric elements to leverage the advantages of both plasmonic and dielectric resonances (Figure 2), often achieving enhanced functionality or performance [8].

- **Classification Based on Phase Control Mechanism**

**Geometric Phase Metasurfaces:** Also known as Pancharatnam-Berry phase metasurfaces,

these control the phase of circularly polarized light through the orientation angle of anisotropic meta-atoms. The geometric phase is proportional to twice the rotation angle, enabling a complete 2π phase coverage through a 180° rotation. [9]

**Resonant Phase Metasurfaces:** These utilize resonant structures whose dimensions determine the phase response, typically achieving phase control through the variation of structural parameters like size, shape, or spacing. [10]

**Propagation Phase Metasurfaces:** In these designs, the phase accumulation occurs as waves propagate through or along structures of varying optical path lengths, such as nanopillars of different heights [11].

- **Classification Based on Functionality**

**Reflective Metasurfaces:** Designed to manipulate reflected waves, often including a ground plane or reflective layer beneath the meta-atoms. These include metasurface reflectarrays, which can shape reflected wavefronts for beam focusing or beam steering.

**Transmissive Metasurfaces:** Engineered to control transmitted waves, allowing for applications like flat lenses, beam deflectors, and holograms.

**Absorptive Metasurfaces:** Specialized to maximize absorption of incident waves, useful for applications in stealth technology, thermal emitters, and photodetection.

**Bianisotropic Metasurfaces:** These exhibits coupling between electric and magnetic responses, enabling more sophisticated wave manipulation capabilities, including polarization control and asymmetric transmission.

- **Classification Based on Tunability**

**Static Metasurfaces:** These have fixed electromagnetic properties determined during fabrication, offering simplicity but limited to single-function operation.

**Reconfigurable/Tunable Metasurfaces:** Incorporating active elements or responsive materials to dynamically alter their electromagnetic properties, as shown in Figure 3. These can be further categorized based on their tuning mechanism:

a) **Mechanically Tunable:** Using physical deformation, MEMS, or other mechanical means to reconfigure the metasurface structure
b) **Electrically Tunable:** Incorporating components like varactor diodes, liquid crystals, or graphene that respond to applied voltages
c) **Optically Tunable:** Using photosensitive materials whose properties change

under illumination

d) **Thermally Tunable:** Exploiting temperature-dependent material properties to control the metasurface response

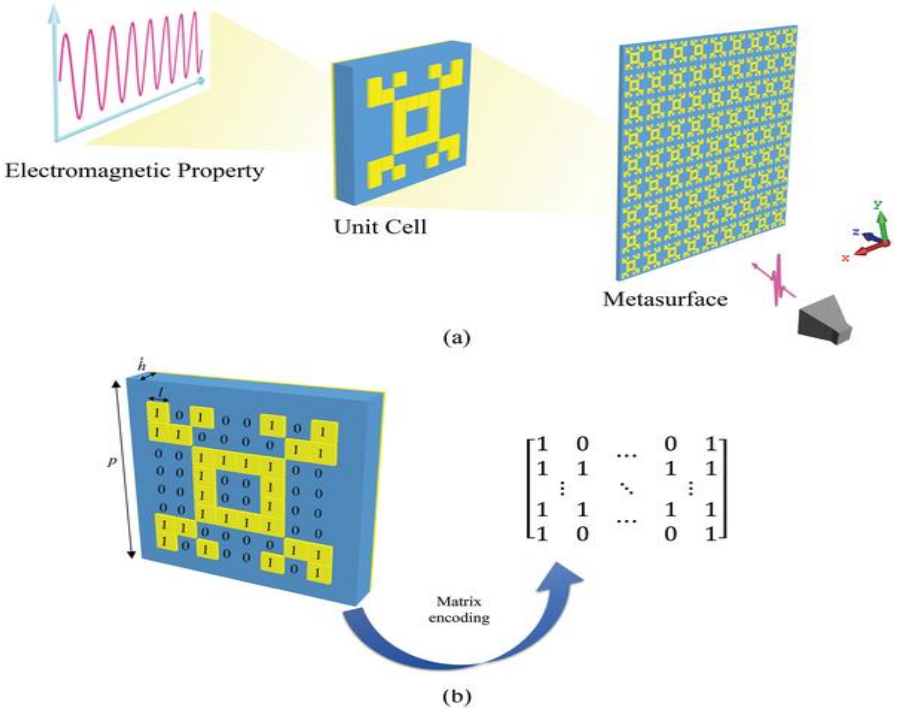


Figure 3: Reconfigurable metasurface: (a) Schematic illustration of the metasurface structure; (b) Illustration of the tuning mechanism where external stimuli modify the electromagnetic properties of the meta-atoms *[12]*.

The diversity of metasurface types reflects the remarkable versatility of this technology and the wide range of approaches that can be employed to achieve specific electromagnetic functions. Each type offers distinct advantages and limitations, making the selection of the appropriate metasurface design crucial for any given application.

### I.2.2 Applications

Metasurfaces have demonstrated exceptional versatility across a wide spectrum of applications, revolutionizing how we manipulate electromagnetic waves. Their unique ability to control wave properties at subwavelength scales has enabled numerous innovative technologies spanning from microwave to optical frequencies.

- **Telecommunications and Wireless Communications**

Metasurfaces are increasingly recognized as transformative elements in next-generation wireless communication systems, particularly for 5G and future 6G networks. Their ability to manipulate electromagnetic waves with unprecedented precision offers solutions to many challenges in the telecommunications industry, as summurized in figure 4 [13].

**Intelligent Reflecting Surfaces (IRS):** One of the most promising applications of metasurfaces in telecommunications is their implementation as intelligent reflecting surfaces that can enhance signal coverage in non-line-of-sight scenarios. These surfaces can be programmed to redirect signals around obstacles, effectively creating virtual line-of-sight paths between transmitters and receivers [14].

**Beamforming and Beam Steering:** Reconfigurable metasurfaces enable dynamic beam steering and beamforming, allowing for precise targeting of electromagnetic energy. This capability is crucial for millimeter-wave communications in 5G and 6G systems, where narrow beams are required to overcome path loss and maximize signal strength.

**Mimo Enhancement:** Metasurfaces can improve MIMO (Multiple-Input Multiple-Output) system performance by creating rich multipath environments and controlling channel characteristics. They can also serve as low-profile, efficient MIMO antenna arrays with beam diversity capabilities.

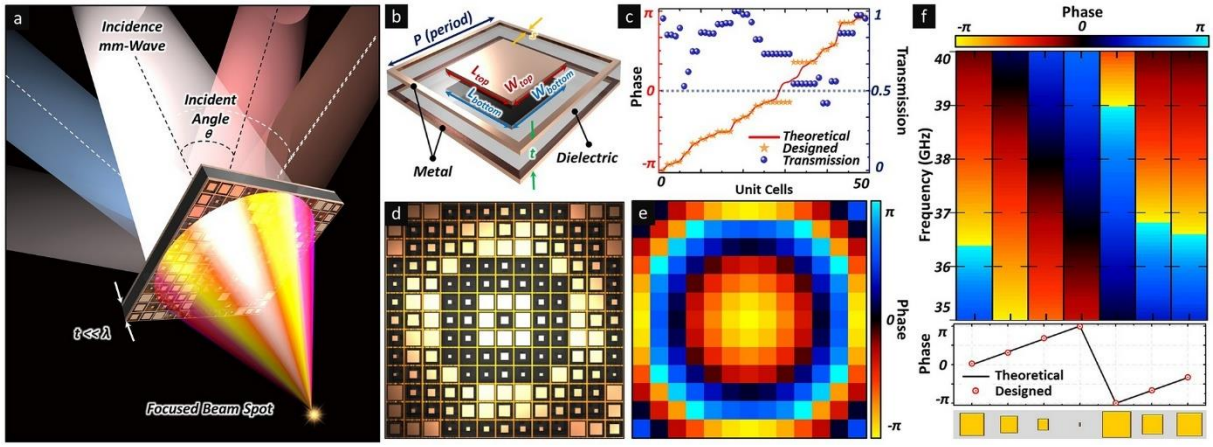


Figure 4: Implementation of metasurfaces in next-generation wireless communication systems *[15]* .

- **Antenna Applications**

**Metasurface Antennas:** Metasurfaces have enabled the development of ultrathin, high-performance antennas with capabilities exceeding conventional designs. Holographic metasurface antennas, which modulate surface impedance to create complex radiation patterns,

have demonstrated high gain and circular polarization [16].

**Reflectarrays and Transmitarrays:** Metasurface-based reflectarrays combine the focusing capabilities of parabolic reflectors with the low profile of printed arrays. Similarly, transmitarray metasurfaces can focus and redirect transmitted waves without the bulk of traditional lenses.

**Huygens' Metasurface Antennas:** These specialized antennas leverage both electric and magnetic responses to achieve high radiation efficiency and tailored radiation patterns. Their ability to minimize back-radiation makes them particularly valuable for applications requiring unidirectional emission [17].

- **Wavefront Engineering and Optical Applications**

**Metalenses:** Metasurfaces have revolutionized optics by enabling flat lenses (metalenses) that can focus light without the bulk of traditional refractive optics. These ultrathin optical elements can be designed to overcome classical aberrations and achieve diffraction-limited focusing [18].

**Holography:** Metasurface holograms can generate complex 3D images with high efficiency and resolution. Unlike conventional holograms, metasurface implementations can work with a single wavelength, control polarization, and even create multiplexed images that respond differently to various illumination conditions [19].

**Polarization Control:** Metasurfaces excel at manipulating the polarization state of electromagnetic waves, enabling functions like polarization conversion, circular polarizers, and waveplates. These capabilities are crucial for numerous applications in sensing, communications, and imaging.

- **Sensing and Imaging**

**Biosensors:** The strong field confinement and sensitivity to environmental changes make metasurfaces excellent platforms for biosensing applications. They can detect minute changes in refractive index caused by molecular binding events, enabling label-free, high-sensitivity biosensors.

**Spectral Filters and Detectors:** Metasurfaces can function as highly selective spectral filters or enhance the performance of photodetectors by increasing light absorption in specific wavelength ranges. These capabilities are valuable for spectroscopy, imaging, and sensing applications.

**Computational Imaging:** By encoding specific mathematical operations into their structure,

metasurfaces can perform analog computing on incoming wavefronts, enabling novel approaches to computational imaging and signal processing.

- **Advanced and Emerging Applications**

**Non-Linear Metasurfaces:** By incorporating non-linear materials or designing geometries that enhance non-linear responses, metasurfaces can enable functions like frequency conversion, harmonic generation, and intensity-dependent behavior. These non-linear effects expand the functional range of metasurfaces beyond linear wave manipulation.

**Quantum Metasurfaces:** At the intersection of metasurfaces and quantum optics, quantum metasurfaces can manipulate quantum states of light, potentially enabling new quantum technologies for secure communications and quantum computing.

**Cloaking and Illusion Devices:** Metasurfaces can manipulate scattered fields to reduce an object's radar cross-section or create electromagnetic illusions, making objects appear to have different electromagnetic signatures than their physical reality.

The remarkable diversity of metasurface applications continues to expand as researchers develop new designs, materials, and fabrication techniques. The ability to engineer virtually any electromagnetic response at the subwavelength scale promises to revolutionize numerous technological domains, from telecommunications to quantum information processing, in the coming decades.

## I.3 Characteristic Mode Analysis (CMA)

Characteristic Mode Analysis (CMA) is technique that provides a powerful framework for analyzing the electromagnetic behavior of conducting bodies by decomposing the total current into a set of orthogonal modal currents. Originally introduced by Garbacz [20] and later refined by Harrington and Mautz [21], CMA offers valuable physical insights into radiation and scattering phenomena.

At its core, CMA is based on the eigenvalue decomposition of the impedance operator that relates the electric field to the induced current on a conducting surface. The governing equation of characteristic mode decomposition can be expressed as [22]:

$$X(J_n) = \lambda_n R(J_n) \#(2)$$

where X and R represent the imaginary and real parts of the impedance operator Z, respectively, $J_n$ represents the characteristic current mode, and $\lambda_n$ is the corresponding eigenvalue. This formulation constitutes a generalized eigenvalue problem, which can be solved numerically to

obtain a set of characteristic modes and their associated eigenvalues.

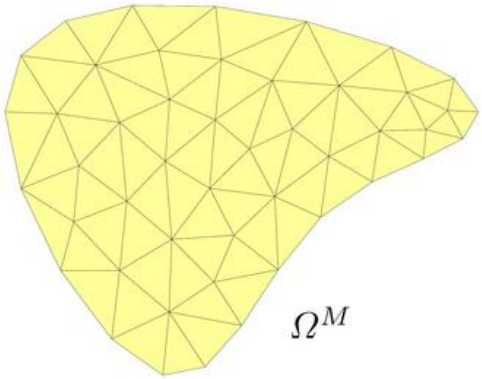


Figure 5:Example of a scatterer's triangular (Delaunay) discretization for numerical solution of the characteristic mode eigenvalue problem *[23]*.

The impedance operator Z is defined by the relationship between the incident electric field and the induced current on the conductor's surface:

$$Z(J) = \hat{n} \times \hat{n} \times E^s(J) \#(3)$$

where n̂ is the unit normal to the surface, and $E^s$ is the scattered electric field produced by the current J.

The numerical solution of the CMA eigenvalue problem typically involves discretizing the conducting body into small elements and applying methods like the Method of Moments (MoM) to convert the operator equation into a matrix equation:

$$[X][I_n] = \lambda_n[R][I_n] \#(4)$$

where [X] and [R] are the discretized versions of the imaginary and real parts of the impedance matrix [Z], and $[I_n]$ represents the expansion coefficients of the n-th characteristic mode current. The eigenvalues $\lambda_n$ have significant physical meaning—they represent the ratio of reactive power to radiated power for each mode. When $\lambda_n = 0$, the mode is at resonance, indicating equal storage of electric and magnetic energy. Positive eigenvalues ($\lambda_n > 0$) indicate inductive modes where magnetic energy storage dominates, while negative eigenvalues ($\lambda_n < 0$) correspond to capacitive modes with dominant electric energy storage [24].

A useful parameter derived from the eigenvalue is the modal significance (MS), defined as:

$$MS_n n = \left| \frac{1}{1 + j\lambda_n} \right| \#(5)$$

Modal significance ranges from 0 to 1, with values close to 1 indicating strongly resonant modes that contribute significantly to radiation or scattering. The characteristic angle, another important parameter, is defined as:

$\alpha_n = 180° - tan - 1(\lambda_n) \#(6)$ characteristic angle of 180° corresponds to a resonant mode, while angles approaching 90° or 270° indicate highly reactive modes that store predominantly electric or magnetic energy, respectively [25].

One of the most valuable properties of characteristic modes is their orthogonality. The farm fields produced by different characteristic modes are orthogonal to each other, making them an ideal basis for representing the radiation pattern of a complex structure. Additionally, when excited properly, each mode can contribute independently to the total radiation, allowing for systematic antenna design and optimization [26].

The total current on a conducting body can be expressed as a weighted sum of the characteristic mode currents:

$$J = \sum_n \alpha_n . J_n \#(7)$$

where $\alpha_n$ are the modal excitation coefficients. These coefficients depend on how well the excitation source (such as a voltage source or incident field) couples to each characteristic mode, providing valuable insights for optimal feeding of antennas [27].

Characteristic Mode Analysis thus provides a rigorous mathematical framework with clear physical interpretation, enabling engineers to understand the fundamental electromagnetic behavior of conducting structures. This understanding forms the basis for systematic antenna design approaches that will be explored in subsequent sections.

### I.3.1 Methodologies of Analysis

The practical implementation of Characteristic Mode Analysis involves several methodological approaches and computational techniques. This section explores the key methodologies used in CMA, from numerical formulation to specialized analysis techniques.

- **Numerical Implementation**

**Method of Moments Formulation:** The most common approach to solve the CMA eigenvalue problem employs the Method of Moments (MoM) with the Electric Field Integral Equation (EFIE). This involves discretizing the structure into small elements and expanding the current using basis functions, typically Rao-Wilton-Glisson (RWG) basis functions for arbitrarily shaped 3D structures [28].

The impedance matrix elements are computed as:

$$Z_{mn} = \int \quad f_m(r) \cdot [L(f_n)(r)]dS\#(8)$$

where $f_m$ and $f_n$ are basis functions, and L is the integral operator that relates current to electric field. The impedance matrix is then separated into its real and imaginary parts to form the generalized eigenvalue problem.

**Eigenvalue Decomposition Techniques:** Several numerical methods are available for solving the generalized eigenvalue problem, including the Schur decomposition, Arnoldi iteration, and QZ algorithm. For electrically large structures, specialized techniques like the Implicitly Restarted Arnoldi Method (IRAM) or the Jacobi-Davidson algorithm may be employed to efficiently compute a subset of the characteristic modes.

- **Modal Tracking**

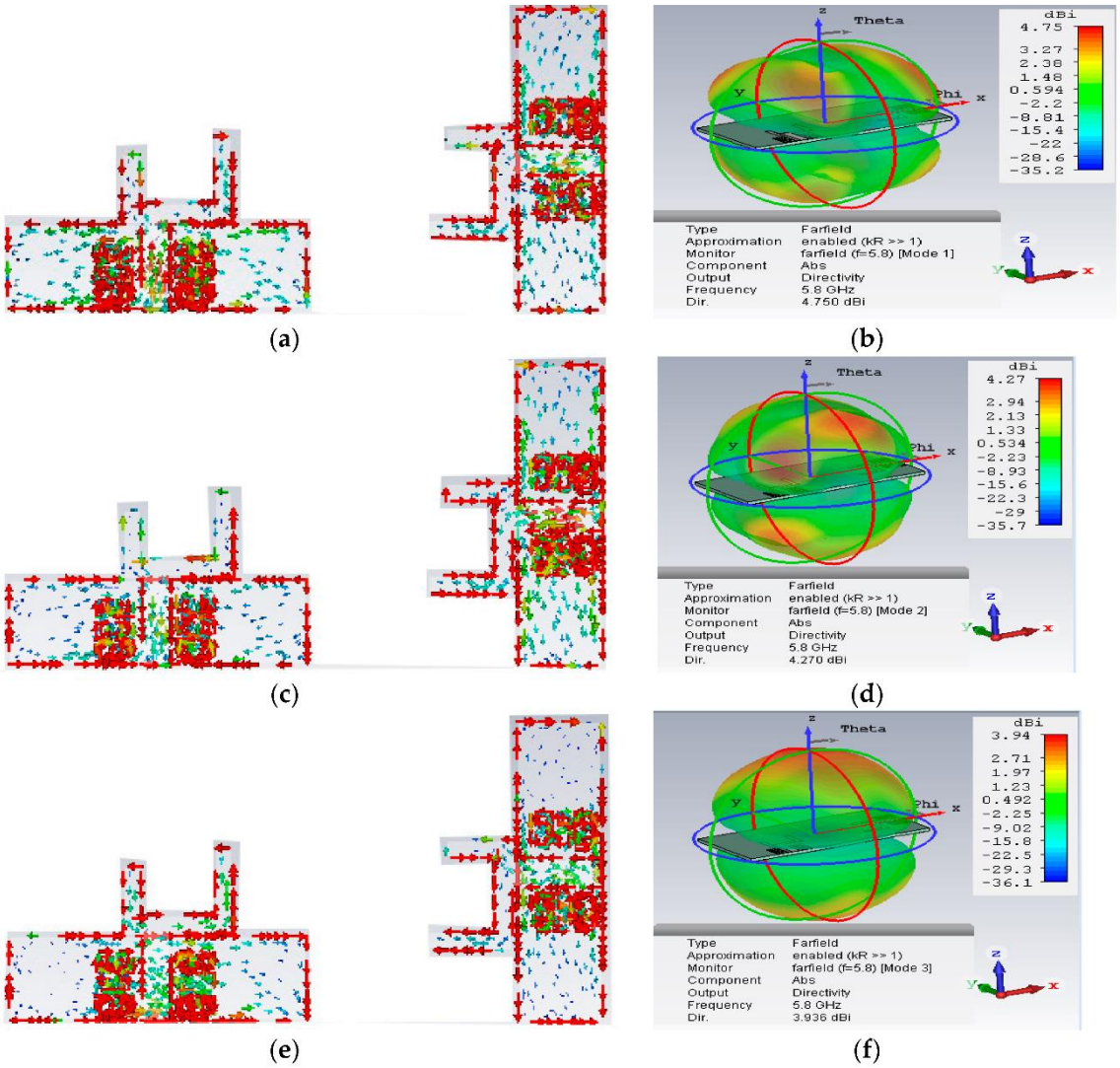


Figure 6: Characteristic angle tracking across frequency for multiple modes. *[29]*

One of the challenges in CMA is tracking modes across frequency, as the eigenvalue ordering may change with frequency, see Figure 6. Various modal tracking methods have been developed to maintain consistency in modal analysis across the frequency spectrum:

**Correlation-Based Tracking:** This approach calculates correlation coefficients between mode currents or far fields at adjacent frequency points, assigning the same mode index to highly correlated solutions.

**Eigenvalue-Based Tracking:** Exploiting the continuous nature of eigenvalue curves, this method predicts eigenvalue trajectories to identify corresponding modes at different frequencies.

**Modal Significance-Based Tracking:** Similar to eigenvalue tracking but using modal significance, which often produces smoother curves that are easier to track.

- **Extended CMA Formulations**

Several extensions to the basic CMA have been developed to address specific challenges and broaden its applicability:

**Surface Formulation for Material Bodies:** Extended CMA formulations allow for the analysis of dielectric and magnetic bodies, not just perfect electric conductors. This involves using a surface integral equation formulation with equivalent electric and magnetic currents.

**Volume Integral Equation CMA:** For inhomogeneous dielectric bodies, volume integral equation formulations may be used, discretizing the volume rather than just the surface.

**Combined Field Integral Equation CMA:** To address low-frequency breakdown issues in the standard EFIE formulation, Combined Field Integral Equation (CFIE) based CMA has been developed, combining electric and magnetic field integral equations.

- **Computational Efficiency Techniques**

As the electrical size of the analyzed structure increases, computational demands grow rapidly. Several approaches have been developed to improve computational efficiency:

**Fast Multipole Method (FMM):** For electrically large structures, the Multi-Level Fast Multipole Algorithm (MLFMA) can be incorporated into CMA to reduce computational complexity from $O(N^2)$ to O (N log N), where N is the number of unknowns.

**Model Order Reduction:** Techniques like the Adaptive Cross Approximation (ACA) or Proper Orthogonal Decomposition (POD) can be used to create reduced-order models that capture the essential characteristics of the full problem with lower computational cost.

**GPU Acceleration:** Many CMA implementations utilize Graphics Processing Units (GPUs) to

parallelize computationally intensive tasks, particularly the matrix operations required for the eigenvalue decomposition.

- **Analysis Techniques**

Beyond the basic computation of characteristic modes, several specialized analysis techniques have been developed to extract meaningful insights:

**Modal Excitation Analysis:** This involves calculating modal weighting coefficients to determine how effectively a given excitation source (such as a voltage source or incident plane wave) couples to each characteristic mode.

**Modal Expansion of Radiated Fields:** The far field pattern can be decomposed into contributions from individual characteristic modes, allowing engineers to identify which modes are responsible for specific radiation pattern features.

**Modal Quality Factor Analysis:** By analyzing the frequency derivative of eigenvalues, the modal quality factor (Q) can be determined, providing insights into the bandwidth potential of different modes.

**Group Theory Applications:** Symmetry properties of structures can be exploited using group theory to predict mode behavior, such as eigenvalue degeneracy and modal current patterns, without explicitly solving the full eigenvalue problem.

These methodologies collectively form a robust framework for applying CMA to practical problems in antenna design and electromagnetic analysis. As computational capabilities continue to advance, these techniques are becoming increasingly accessible to engineers and researchers, facilitating the application of CMA to more complex and challenging problems.

## I.3.2 Applications

Characteristic Mode Analysis has emerged as a powerful tool in electromagnetic engineering, offering unprecedented insights into the fundamental behavior of radiating and scattering structures. This section explores the diverse applications of CMA across various domains, with a particular focus on antenna design and optimization.

- **Antenna Design and Optimization**

**Systematic Antenna Design:** CMA provides a physics-based approach to antenna design by revealing the inherent radiation mechanisms of arbitrary structures. Understanding the characteristic modes supported by a structure allows engineers to systematically design antennas with desired radiation properties rather than relying on trial-and-error approaches.

**Optimal Feed Placement:** One of the most valuable applications of CMA is determining optimal feed locations for antennas. By analyzing the modal current distributions, engineers can identify positions where feeding will efficiently excite desired modes while suppressing unwanted ones. Figure 7 represents an example of this application.

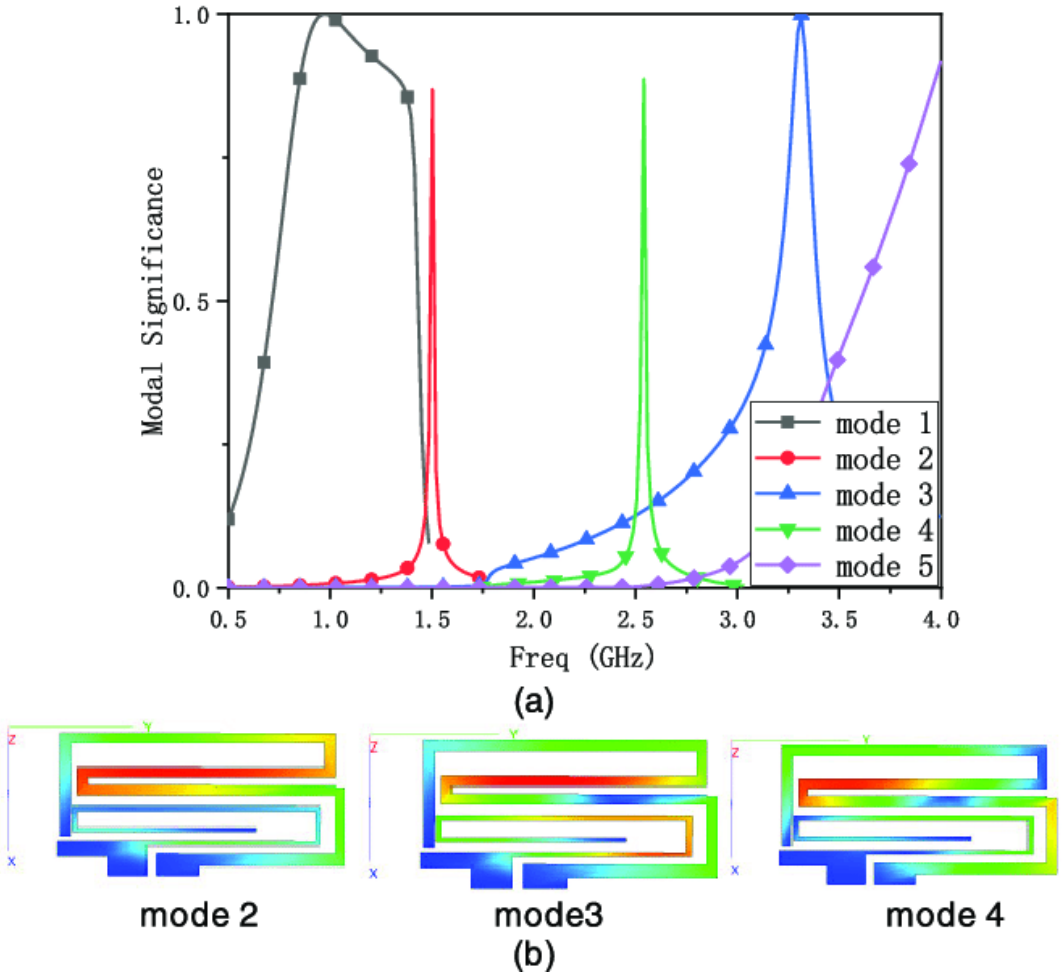


Figure 7:Characteristic mode analysis for optimal feed placement: (a) Modal significance plot showing resonant frequencies of dominant modes; (b) Current distribution of the first characteristic mode indicating optimal feed location at current maxima *[30]*.

**Bandwidth Enhancement:** CMA offers valuable insights for bandwidth enhancement by identifying closely spaced modal resonances that can be combined to create wideband operation. Techniques such as modal manipulation through structural modifications or loading can be used to adjust modal resonances and improve bandwidth.

**Miniaturization Techniques:** By understanding how structural changes affect modal resonances, CMA guides the development of compact antennas. Engineers can strategically

modify structures to lower the resonant frequency of desired modes without significantly increasing the physical size [31].

- **MIMO Antenna Systems**

**Pattern Diversity Design:** The orthogonality of characteristic modes makes CMA particularly well-suited for designing Multiple-Input Multiple-Output (MIMO) antennas with high pattern diversity. By exciting different characteristic modes, multiple radiation patterns with low correlation can be achieved from a single compact structure.

**Isolation Enhancement:** CMA helps identify mechanisms causing coupling between antenna elements in MIMO arrays and guides the development of decoupling structures. By analyzing the characteristic modes of the entire array, engineers can design structures that suppress modes contributing to mutual coupling.

**Compact MIMO Design:** The challenge of integrating multiple antennas in limited space, such as in mobile devices, can be addressed through CMA by leveraging closely spaced yet orthogonal modes. This enables the design of compact MIMO antennas with high efficiency and low correlation.

- **Platform-Integrated Antennas**

**Chassis Mode Utilization:** CMA helps engineers harness the natural resonances of device chassis or vehicle structures as part of the antenna system. Rather than fighting against the electromagnetic influence of the platform, this approach leverages it to enhance radiation performance.

**UAV and Vehicle Antennas:** For unmanned aerial vehicles (UAVs) and other vehicles, CMA enables the design of conformal antennas that efficiently utilize the vehicle structure while maintaining desired radiation characteristics and minimizing aerodynamic impact.

**Wearable and Implantable Antennas:** CMA provides insights into the complex interactions between antennas and biological tissues, guiding the design of efficient wearable and implantable antennas for medical and consumer applications.

- **Advanced Antenna Technologies**

**Reconfigurable Antennas:** CMA facilitates the design of reconfigurable antennas by revealing how loading elements (such as switches, PIN diodes, or varactors) can selectively control different characteristic modes, enabling pattern, polarization, or frequency reconfigurability [31].

**Metasurface Antenna Design:** The combination of CMA with metasurface technology has

led to innovative antenna designs. CMA helps understand the modal behavior of metasurface structures, enabling more efficient and purposeful design of metasurface antennas with tailored radiation properties [32].

**Dielectric Resonator Antennas:** CMA has been extended to analyze dielectric resonator antennas (DRAs), providing insights into the natural resonance modes of dielectric structures and guiding their design for optimal radiation performance.

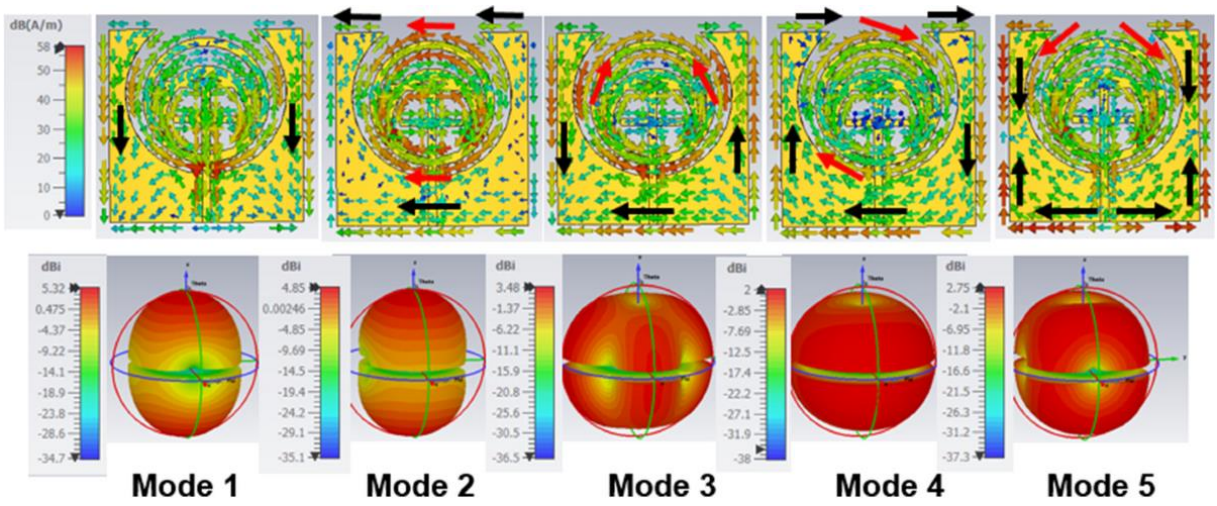


Figure 8:Application of Characteristic Mode Analysis in advanced antenna design *[33]*.

- **Analytical and Computational Applications**

**Radar Cross Section (RCS) Analysis:** CMA provides a modal decomposition of scattered fields, offering insights into the scattering mechanisms of complex objects. This can guide the design of structures with specific scattering properties for radar and stealth applications.

**Educational Tool:** CMA serves as a powerful educational tool, helping students and researchers develop intuition about electromagnetic radiation and scattering phenomena through visual representation of modal currents and their associated fields.

**Computational Electromagnetics Validation:** The orthogonality properties and physical significance of characteristic modes make them valuable for validating computational electromagnetics codes, providing a rigorous benchmark for numerical solutions.

- **Emerging Applications**

**5G and 6G Communications:** CMA is finding increasing application in the design of millimeter-wave antennas for 5G and future 6G systems, where compact multiple-antenna solutions with high efficiency are required to overcome the propagation challenges at high

frequencies.

**Internet of Things (IoT):** For IoT devices, which often have severe constraints on size, power, and cost, CMA enables the design of efficient multiband antennas that can be integrated into compact devices while maintaining good radiation performance.

**Electromagnetic Security:** CMA is being applied to analyze and design structures for electromagnetic security applications, such as RFID systems with controlled reading ranges or antennas with specific radiation patterns to minimize interception.

The wide range of CMA applications continues to expand as researchers develop new analysis techniques and apply them to emerging challenges in electromagnetic engineering. The physics-based insights provided by CMA complement other design approaches, offering a powerful framework for understanding and engineering complex electromagnetic systems.

## I.4 Conclusion

this chapter, we presented the theoretical foundations and key concepts of Metasurfaces (MTS) and Characteristic Mode Analysis (CMA), emphasizing their importance in modern electromagnetic engineering. Metasurfaces enable advanced wave manipulation using compact structures, while CMA offers a systematic approach to understanding and optimizing radiation behavior. Their synergy opens new possibilities in antenna design and next-generation wireless systems. This foundation sets the stage for exploring their practical applications in the following chapters.

# Chapter II

# Numerical Results and

# Discussion

## II.1 Introduction

This chapter introduces metasurface antennas as innovative structures that enable advanced electromagnetic wave control using subwavelength surface elements. Unlike traditional antennas, they offer compactness, beam shaping, and wide or broadband operation. Two key designs are analyzed: a low-profile broadband antenna based on multimode resonance and a wide-beam antenna using complementary source concepts, highlighting their design strategies and performance.

## II.2 Design of Low-Profile Broadband Metasurface Antenna with Multimode Resonance

### II.2.1 Study of Antenna Without MTS

- **Design configuration**

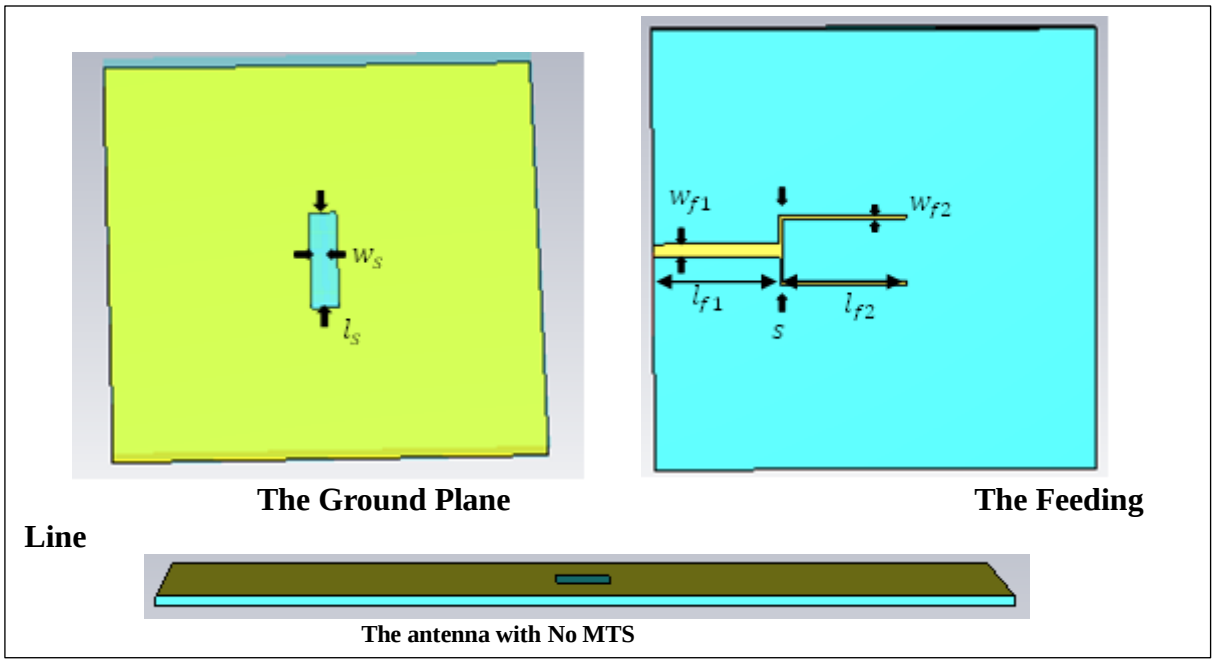


Figure 2:Antenna structure without metasurface

The initial version of the antenna is composed of a microstrip-fed slot structure situated on a

Figure 9 shows the initial design that includes dielectric substrate of dielectric permittivity $\varepsilon_r = 2.65$. The ground plane is printed on the bottom of this substrate. A central slot is etched to serve as the main radiating element. The slot has a rectangular shape and precisely centred to ensure symmetrical excitation. On the other side of substrate, a feeding mechanism is considered, which consists of a fork-like microstrip line. This feeding structure is implemented on the bottom surface of the substrate to couple electromagnetic energy to the slot via proximity coupling. The forked feed includes a main transmission line and two branching arms, designed to enhance matching and radiation efficiency. No metasurface elements are present in this configuration, and the radiation is solely supported by the interaction between the feed and the ground slot. Table 1 summarizes the global layer characteristics of the proposed antenna

Table.1:Configuration of layers and materials of the initial antenna design

| Layer | Material | Function | Key Parameters |
|---|---|---|---|
| Ground Plane | Copper with slot | Ground reference and coupling | Central rectangular slot |
| Substrate | Dielectric ($\varepsilon_r = 2.65$) | Feeding structure support | Low-loss dielectric |
| Feed Structure | Microstrip line | Power delivery | Fork-like divider configuration |

- **Dimensional Parameters**

Table 2 includes the antenna design dimensions that incorporates precise dimensional control to achieve the desired multimode resonance characteristics

Table 2:Dimensional parameters of the proposed antenna without metasurface

| Parameter | Value (mm) | Description |
|---|---|---|
| $w_s$ | 4 | Width of central slot |

| | | |
|---|---|---|
| $l_s$ | 16 | Length of central slot |
| $wf_1$ | 2.2 | Width of main feeding line |
| $wf_2$ | 0.6 | Width of fork arms |
| $lf_1$ | 20 | Length of main feeding line |
| $lf_2$ | 20 | Length of fork arms |

- **$S_{11}$ Parameters Analysis**

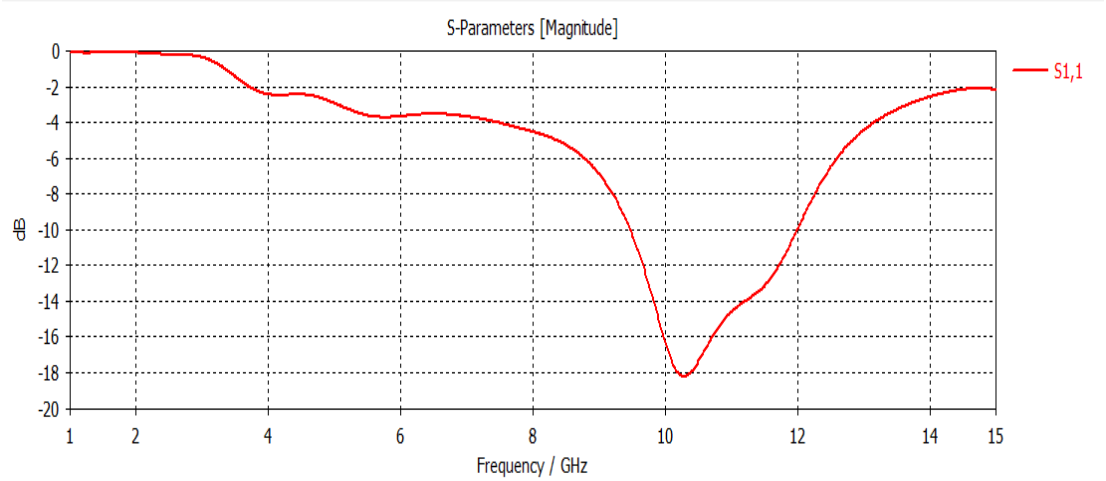


Figure 10: Reflextion coefficient of the slot antenna

The simulated reflection coefficient ($S_{11}$) of the antenna without metasurfaces is depicted in Figure 10. It shows a primary resonance occurring near 10 GHz. At this frequency, the antenna achieves a minimum $S_{11}$ value of approximately −18 dB, indicating a good impedance match. However, the operational bandwidth remains relatively narrow, limiting its performance in wideband applications. These results highlight the need for further optimization to enhance bandwidth and efficiency.

- **Radiation Characteristics**

The radiation performance of the slot antenna without metasurfaces was evaluated at the primary resonance frequency, around 10.32 GHz, where the reflection coefficient reaches its peak.

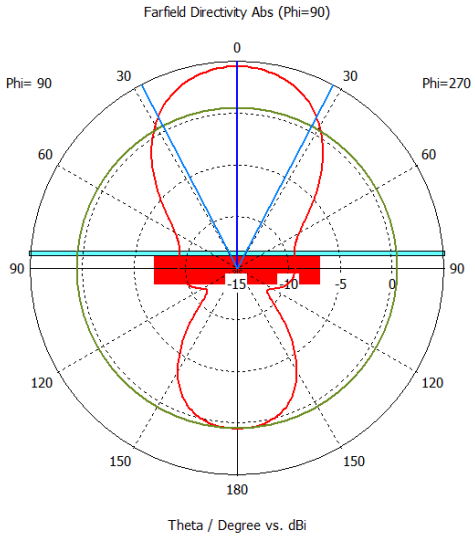


Figure 11:Radiation pattern of antenna without metasurface at 10.32 GHz

Figure 11 illustrates the radiation pattern of the slot antenna at the resonance frequency. At this frequency, the antenna exhibits a bi-directional radiation pattern with a relatively narrow beamwidth.

- **Gain Performance**

The gain performance of the antenna is plotted versue the frequency in following figure (see Figure 12).

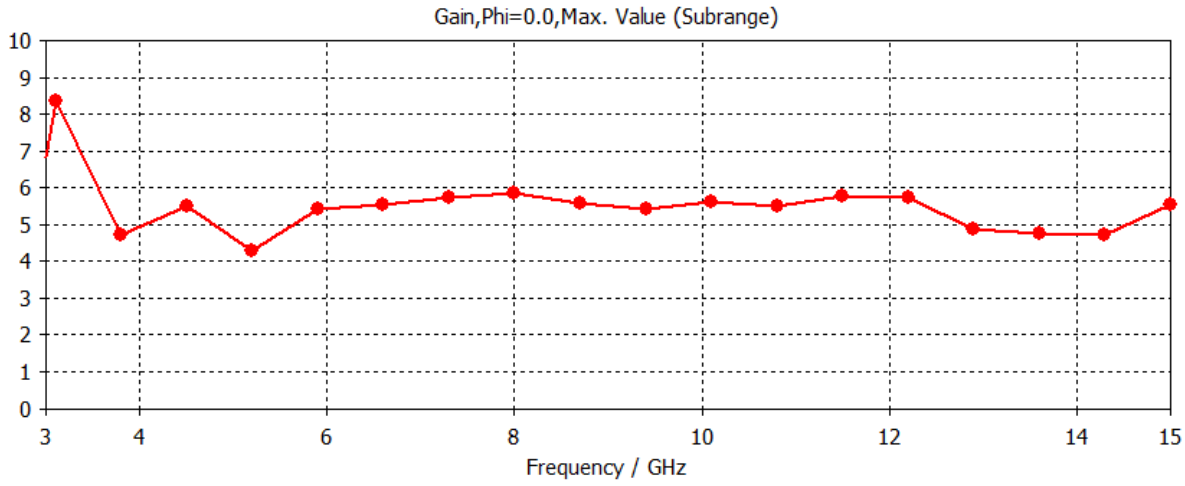


Figure 12:Gain performance curve of slot antenna

The gain curve at the resonance frequency of 10.32 GHz shows a moderate peak gain, with a noticeable variation across the frequency band. While a reasonable gain is achieved at the center

frequency, the overall stability is limited, which reflects the narrow operational effectiveness of the antenna without metasurface enhancement.

- **Performance Limitations Without MTS**
- Limited bandwidth around single resonance
- Low gain across frequency range
- Inconsistent radiation patterns
- Direction instability with frequency
- Moderate directivity performance

### II.2.2 Metasurface (MTS) structure Analysis

- **MTS Design**

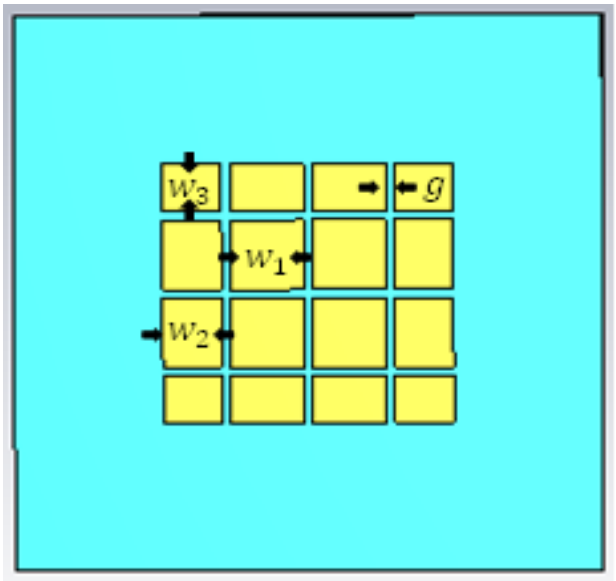


Figure 3:Top view of the metasurface layout with patch

The enhanced antenna design incorporates a non-periodic metasurface (MTS) layer to improve radiation characteristics through multimode resonance. This metasurface is implemented using an array of rectangular copper patches, carefully placed on the top

dielectric substrate. Each patch is dimensioned to interact constructively with the fields radiated from the central slot, enabling optimized surface current distribution and bandwidth enhancement. A top view of the MTS layout showing the patch dimensions ($w_1$, $w_2$, $w_3$) and gap spacing (g) is illustrated in Figure 13, and the specific values are detailed in Table 5.

- **Characteristic Mode Analysis (CMA) of the proposed MTS**

As part of the analysis, Characteristic Mode Analysis (CMA) is carried out to investigate the inherent resonant behavior of the structure. This method provides insight into the natural modes supported by the design, while the Modal Significance (MS) curves help identify which modes are most effective in contributing to radiation. This step is essential for understanding the modal contributions and guiding the optimization process.

The following results, of Table 3, present the CMA performed over multiple frequencies, highlighting several characteristic modes of the structure:

Table 3:CMA of 10 different modes with their 3D radiation patterns and surface current distributions

| **Mode1** | **Mode2** | **Mode3** |
|---|---|---|
| 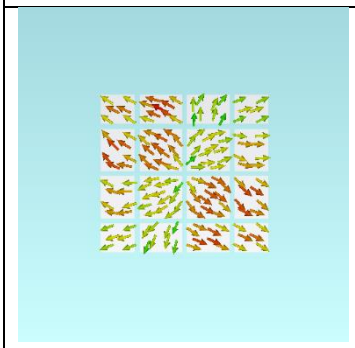 | 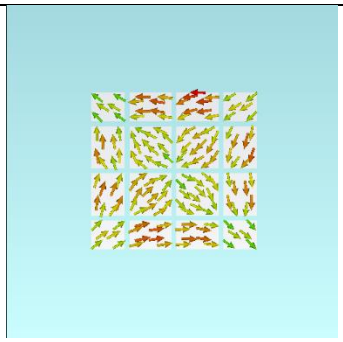 | 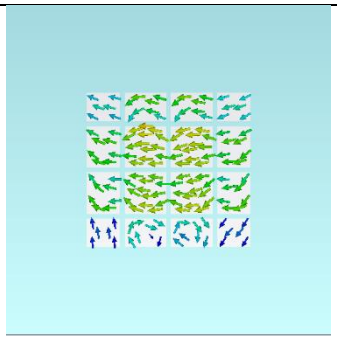 |
| 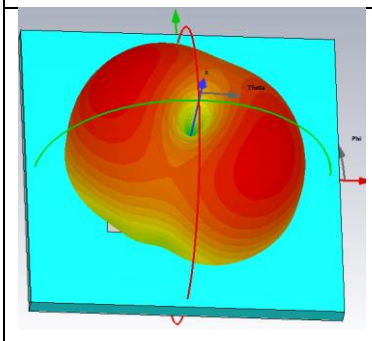 | 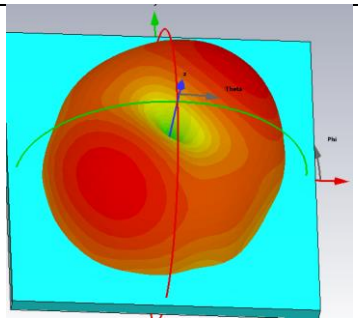 | 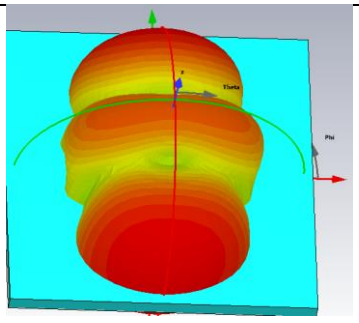 |
| **Mode4** | **Mode5** | **Mode6** |

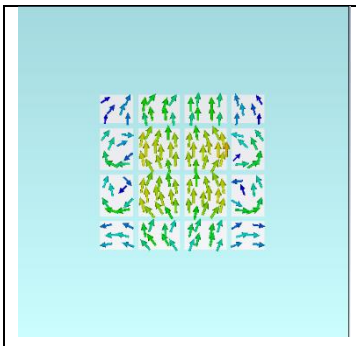

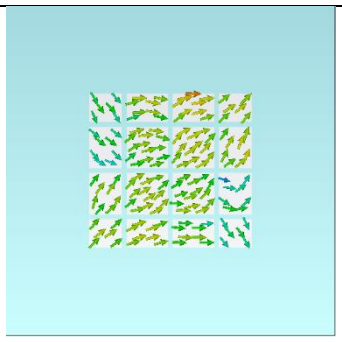

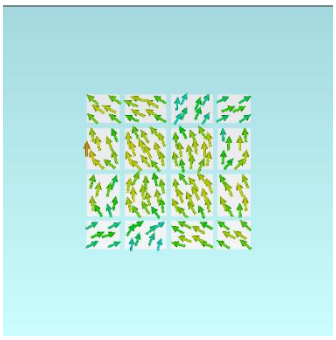

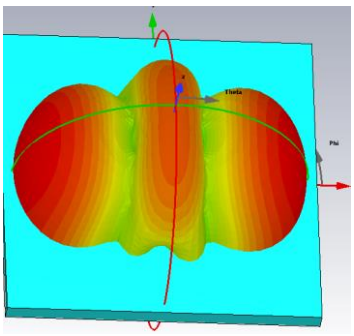

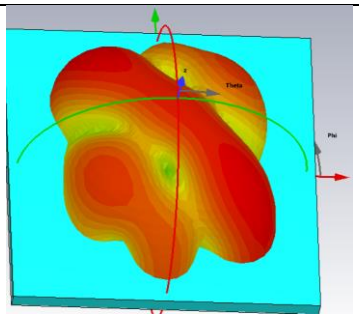

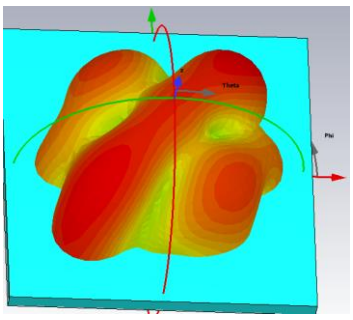

**Mode7** | **Mode8** | **Mode9**

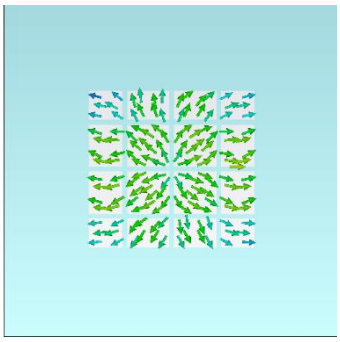

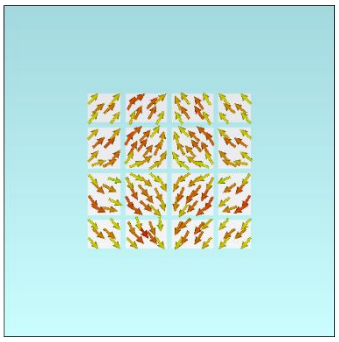

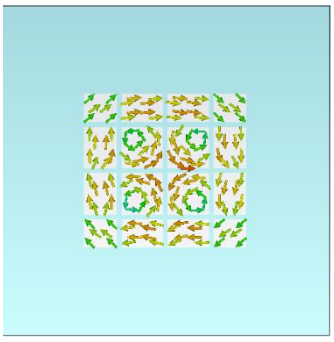

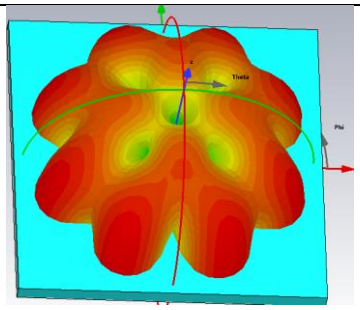

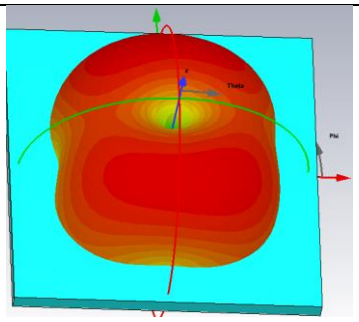

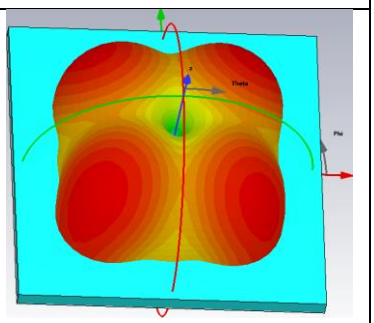

**Mode10**

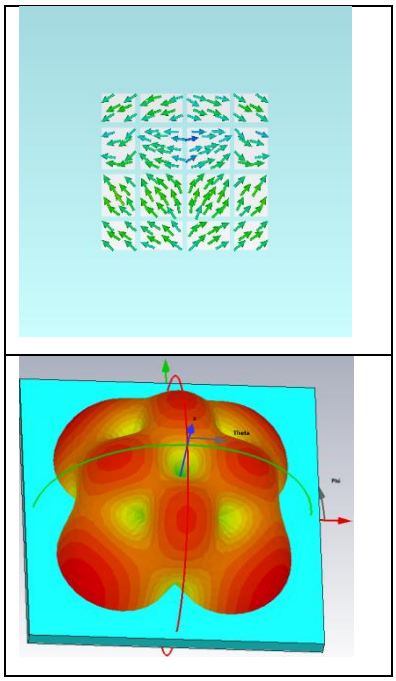

From these results, it can be concluded the following notes;

Surface current distributions at 5.4 GHz for all 10 modes highlight their electromagnetic behavior:

- **Mode 1**: Strong central currents (18.66 dB(A/m)), indicating a dominant resonant mode.
- **Mode 2**: Outer patch dominance (22.08 dB(A/m)), showing effective MTS coupling.
- **Mode 3**: Symmetrical central intensity (20.49 dB(A/m)), supporting broadside radiation.
- **Mode 4**: Balanced distribution (19.60 dB(A/m)), uniform energy spread.
- **Mode 5**: Central focus (18.70 dB(A/m)), highest directivity mode.
- **Mode 6**: Uniform pattern (18.87 dB(A/m)), stable contribution.
- **Mode 7**: Outer strong, inner weak (17.39 dB(A/m)), less focused.
- **Mode 8**: Phase variation (15.97 dB(A/m)), moderate intensity.
- **Mode 9**: Central/outer mix (18.58 dB(A/m)), broad resonance.
- **Mode 10**: Diffuse (15.42 dB(A/m)), wide but weaker distribution.

<The highest current magnitudes (e.g., Mode 2 at 22.08 dB(A/m)) correlate with modes showing strong MTS interaction, reinforcing their selection.

The 3D radiation patterns at 5.4 GHz for all 10 modes reveal varying directivity and lobe structures:

- **Mode 1**: 4.97 dBi, broadside with a single strong lobe.
- **Mode 2**: 5.31 dBi, broadside with slight asymmetry.
- **Mode 3**: 5.23 dBi, multi-lobed pattern.
- **Mode 4**: 5.31 dBi, broadside with enhanced focus.
- **Mode 5**: 5.75 dBi, strongest directivity, broadside.
- **Mode 6**: 5.41 dBi, balanced lobes.
- **Mode 7**: 3.84 dBi, diffuse pattern.
- **Mode 8**: 4.39 dBi, moderate directivity.
- **Mode 9**: 4.37 dBi, multi-lobed with good coverage.
- **Mode 10**: 4.39 dBi, diffuse but broad coverage.

The best modes (1, 2, 5, and 9) exhibit higher directivity (4.97-5.75 dBi) and stable broadside patterns, ideal for wideband applications. Modes 7 and 8 show lower directivity (3.84-4.39 dBi), suggesting less contribution to peak performance.

**Modal Significance (MS) Analysis**

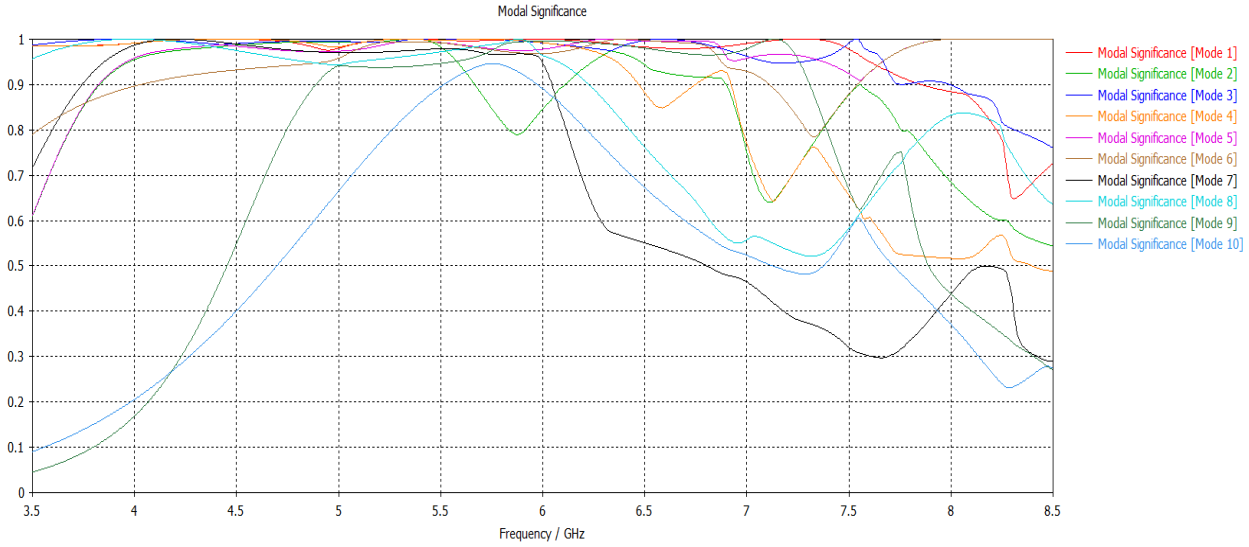


Figure 14: Modal Significance curves showing resonance strength of the 10 modes

Modal Significance (MS) is a key metric in Characteristic Modes Analysis (CMA) that indicates the resonance strength of each mode across a frequency range. MS values range from 0 to 1, where values close to 1 signify strong resonance, making those modes highly significant for antenna design. From Figure 14, the provided MS plot for Modes 9 and 10, along with earlier data for all 10 modes, shows that MS peaks occur around 5.0-5.5 GHz, with Mode 10 reaching near 1.0 at 5.5 GHz and Mode 9 maintaining high significance (~0.9) in the same range. This indicates strong resonant behavior, particularly for these higher-order modes, due to their quasi-degenerate nature, which enhances broadband performance. We selected the best modes (e.g., Modes 1, 2, 9, and 10) based on their high MS values and their contribution to wideband operation, ensuring optimal coupling with the metasurface (MTS) as illustrated in Figure 15.

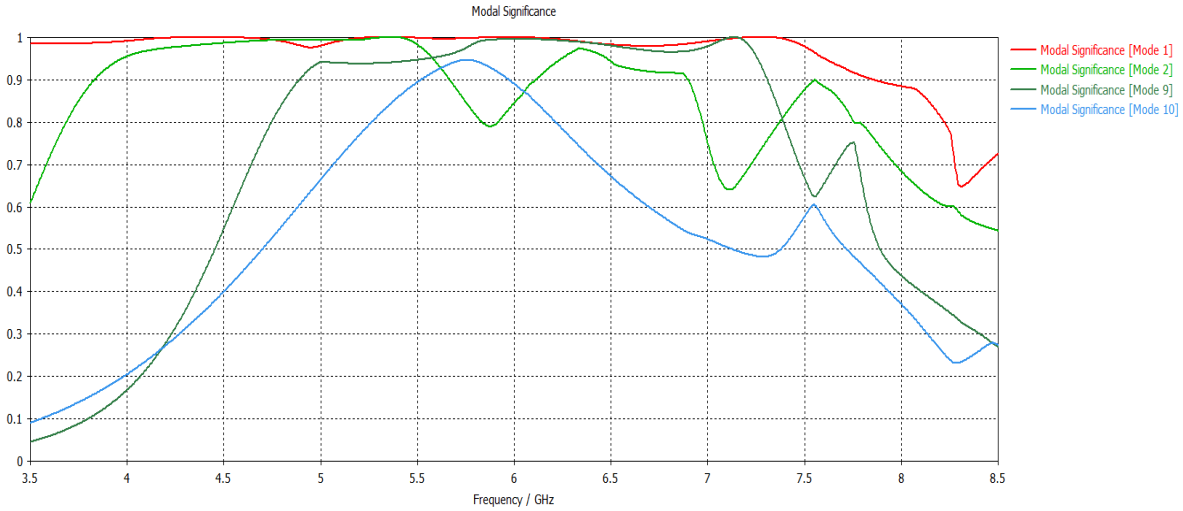


Figure 15:Modal Significance curves of the significant modes

- **Performance of Antenna integrating MTS**

The integration of MTS significantly enhances antenna performance. Without MTS, the antenna exhibits a narrow bandwidth (<30%) with limited resonant modes and a simple broadside pattern with higher cross-polarization. With MTS, the bandwidth exceeds 79% due to multimode resonance, leveraging the high MS modes (1, 2, 9, 10) to achieve multiple resonant dips (e.g., 3.7, 4.6, 5.4, 5.8, 6.0, 6.7, 7.5 GHz). The radiation pattern improves with directivity ranging from 3.84 to 5.75 dBi, and cross-polarization is reduced to ~ -30 dB, enhancing gain and pattern stability. The MTS, guided by CMA, optimizes current distributions and mode coupling, resulting in a low-profile, broadband antenna ideal for modern wireless applications.

### II.2.3 Study of Antenna integrated with Metasurface (MTS)

- **Design and Structure**

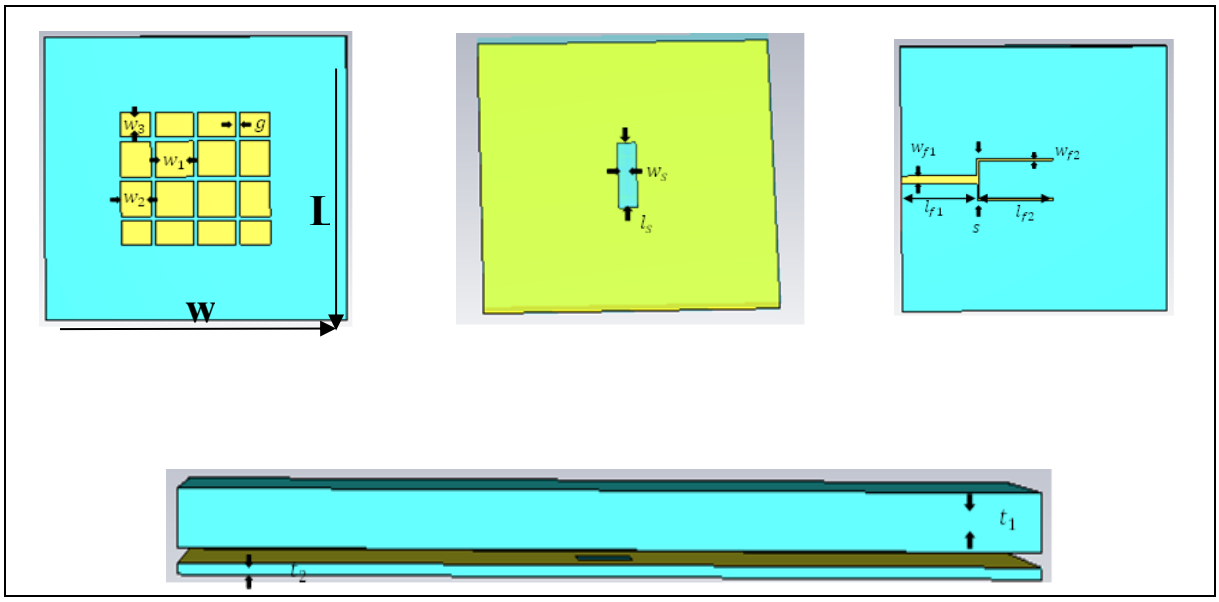


Figure 16:Enhanced antenna structure with metasurface

The enhanced version of the antenna incorporates a non-periodic metasurface layer placed above the ground plane to improve the radiation performance. The full structure consists of three layers: a top dielectric substrate, a ground plane with a central slot, and a bottom dielectric substrate that houses the feeding network. The top dielectric substrate supports an array of metallic patches forming the metasurface, which plays a key role in achieving broadband operation through multimode resonance. The central slot etched in the ground plane is retained from the original design and is used to excite the structure. Energy is fed through a fork-shaped microstrip line printed on the underside of the bottom substrate. The inclusion of the metasurface significantly enhances bandwidth and gain by supporting multiple resonant modes that interact constructively with the slot excitation.

Table 4:Specification of materials for the antenna enhanced by metasurface

| **Component** | **Material** |
|---|---|
| **Top Substrate** | Taconic (εr = 3.5) |
| **Metasurface Patches** | Copper |
| **Ground Plane** | Copper |
| **Bottom Substrate** | Taconic (εr = 2.65) |
| **Feeding Structure** | Copper |

- **Dimensional Parameters**

The antenna design employs precise dimensional tuning to achieve the intended multimode resonance characteristics.

Table 5:Dimensional parameters of the antenna with metasurface

| $w_1$ | $w_2$ | $w_3$ | $g$ | $l_{f1}$ |
|---|---|---|---|---|
| 8.8 | 6 | 7 | 1 | 20 |
| $l_{f2}$ | $w_{f1}$ | $w_{f2}$ | $l_s$ | $w_s$ |
| 20 | 2.2 | 0.6 | 16 | 4 |
| $s$ | $t_1$ | $t_2$ | **L** | **W** |
| 11.2 | 4 | 0.8 | 70 | 70 |

- **$S_{11}$ Parameter**

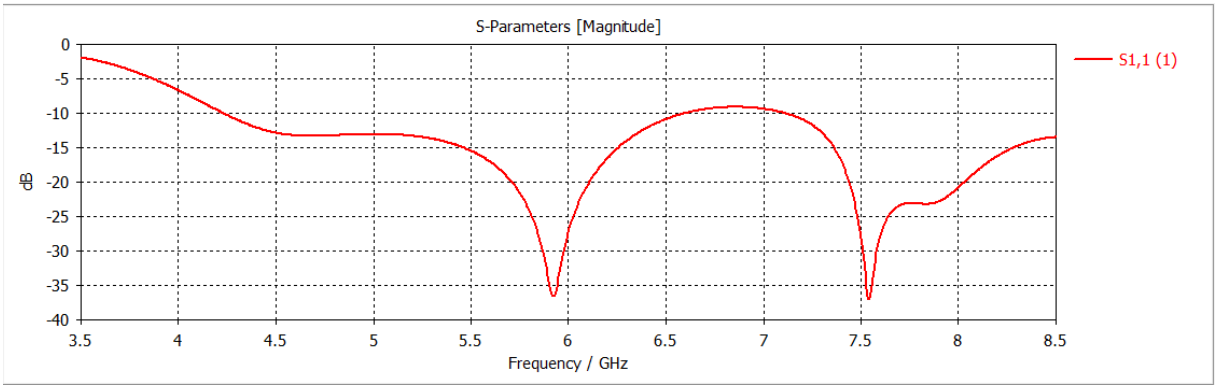


Figure 17: $S_{11}$ response of the integrated antenna with MTS

As illustrated in Figure 17, the $S_{11}$ performance of the antenna with metasurfaces demonstrates a significant enhancement in impedance matching and bandwidth. A strong primary resonance is observed around 6 GHz with a reflection coefficient of approximately −35 dB, followed by a secondary resonance near 7.5 GHz reaching −39 dB. This dual-resonance behavior contributes to a much broader operating bandwidth. Furthermore, the resonance frequencies are shifted to the lower frequencies (from 10 GHz to 5.8 GHz) that leads to achieve high miniaturization. These improvements confirm the effectiveness of the metasurface in enabling multimode operation.

- **Radiation Characteristics**

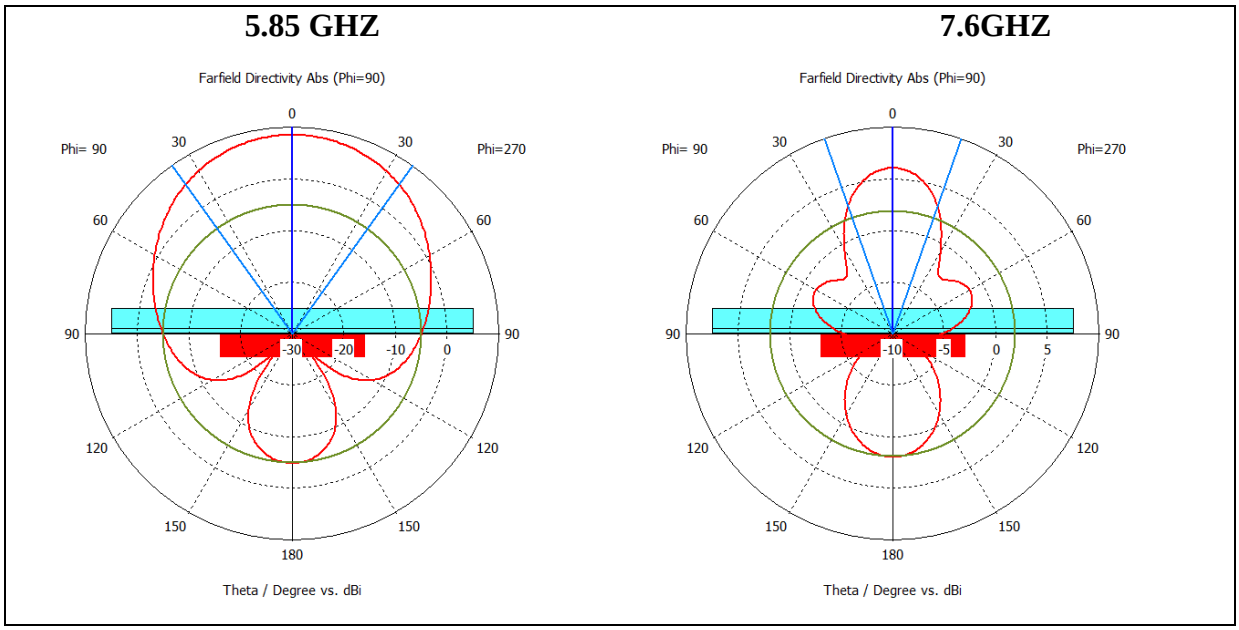


Figure 18:Radiation patterns at; (a) 5.85 GHz and (b) 7.6 GHz

At the radiation pattern is calculated and plotted in Figure 18, at the two resonant frequencies including; 5.85 GHz and 7.6 GHz. It can be seen that the antenna with metasurfaces demonstrates strong and stable radiation performance. At 5.85 GHz, a peak gain of 8.49 dBi is achieved with a broadside direction (0°) and a 3 dB beamwidth of 70.8°, indicating excellent coverage. At 7.6 GHz, the gain remains high at 6.29 dBi with the same broadside direction and a narrower 3 dB beamwidth of 41.9°. These results confirm the metasurface's effectiveness in maintaining both high gain and directional consistency across the extended bandwidth

- **Gain Performance**

The Gain curve, spanning Frame numbers from approximately 3.3816 to 7.162, shows an overall upward trend in the "Gain, Phi=0.0, Max. Value (Subrange)" from around 6.5 to a peak near 9.5. The value remains relatively stable between 7 and 7.5 from frames 4 to 6, with noticeable increases and fluctuations, particularly a sharp rise towards the end. This pattern could correlate with the $S_{11}$ performance improvements, such as the resonance shifts and enhanced bandwidth around 6-7.5 GHz, suggesting improved gain as the antenna's performance optimizes.

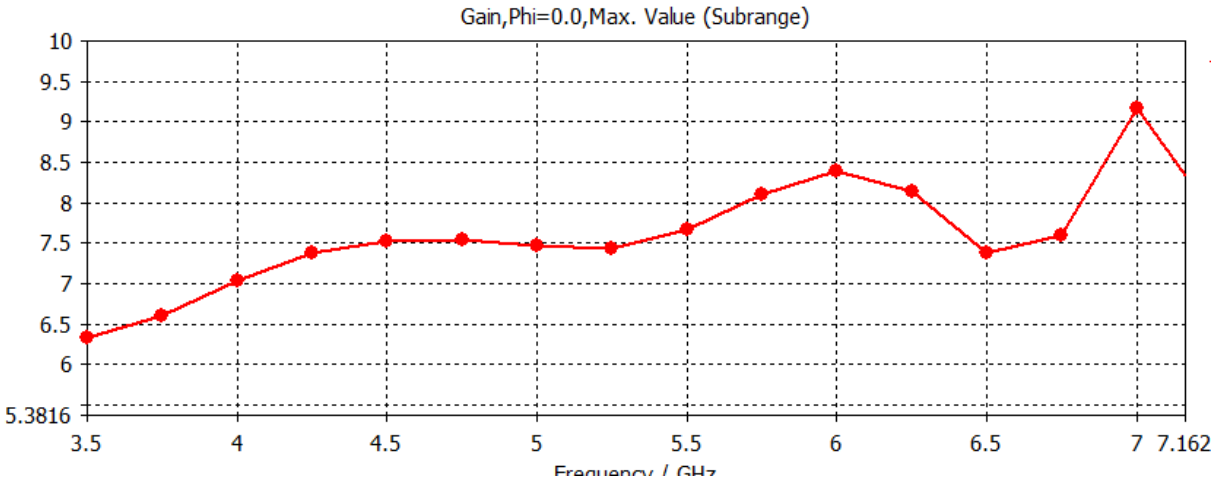


Figure 4: the Gain Performance of the antenna with MTS

## II.2.4 Comparative Analysis: With vs Without Metasurface

- **$S_{11}$ Parameter**

Table 6:Comparative performance analysis $S_{11}$

| Parameter | Without Metasurface | With Metasurface |
|---|---|---|
| **Resonance Frequency** | Single resonance at ~10.32 GHz | Dual resonances at ~6 GHz (−35 dB) and ~7.5 GHz (−39 dB) |
| **Minimum $S_{11}$** | −18 dB | −39 dB |
| **Impedance Bandwidth** | Narrow, centered around 10.32 GHz | Wide bandwidth exceeding 79%<br>Shifted to lower frequencies (Miniaturization) |
| **Matching Quality** | Acceptable near resonance only | Strong and stable matching across wide frequency range |
| **Operation Behavior** | Single-mode operation | Multimode operation enabled by metasurface |

From the table 6, compared to the version without metasurfaces, the antenna with MTS achieves a fourfold improvement in bandwidth, expanding from narrowband operation to over 79%. The reflection coefficient is also improved by more than 20 dB, reflecting significantly enhanced impedance matching. Additionally, the antenna transitions from single-band to dual-band

operation, enabled by the presence of multiple resonant modes.

- **Radiation Pattern**

The radiation pattern of the antenna without metasurfaces is less stable, with poor directionality and broader beam shapes. Beam control varies significantly across the band. With the addition of metasurfaces:

- Side lobe suppression is improved
- Beam direction is stabilized at broadside (0°)
- Beamwidth is well controlled, e.g., 70.8° at 5.85 GHz and 41.9° at 7.6 GHz
- Front-to-back ratio is improved, producing cleaner radiation

These changes indicate a more efficient and directive radiation profile due to the metasurface design.

- **Gain Performance**

Compared to the version without metasurfaces, the antenna with MTS achieves significantly improved and more stable gain performance.

- **Without MTS**, gain varies from **0.86 dBi** to a maximum of **5.52 dBi**, with noticeable fluctuations across frequency.
- **With (MTS**),the gain consistently exceeds **6.5 dBi**, peaking near **9.5 dBi** at around **7.16 GHz** and remaining stable between **7** and **7.5 dBi** from **4** to **6 GHz**.

This gain stability reflects better energy radiation and modal control due to the metasurface integration.

## II.3 Design of A Low-Profile Wide Beam Metasurface Antenna

### II.3.1 Initial Antenna Design (Without Metasurface)

- **Design and Structure**

Figure 20 shows the initial antenna configuration that consists of a two-layer structure comprising a ground plane with a slot and a feeding microstrip line placed on the opposite side of the dielectric substrate. The ground plane features a centrally etched rectangular slot designed to radiate by coupling energy from the microstrip line. The feeding line is printed directly on the bottom surface of the substrate and aligned below the slot to ensure efficient excitation. No

metasurface or additional elements are introduced at this stage. The structure is compact and exhibits a low profile, making it suitable for space-constrained environments where a simple wide-beam solution is required.

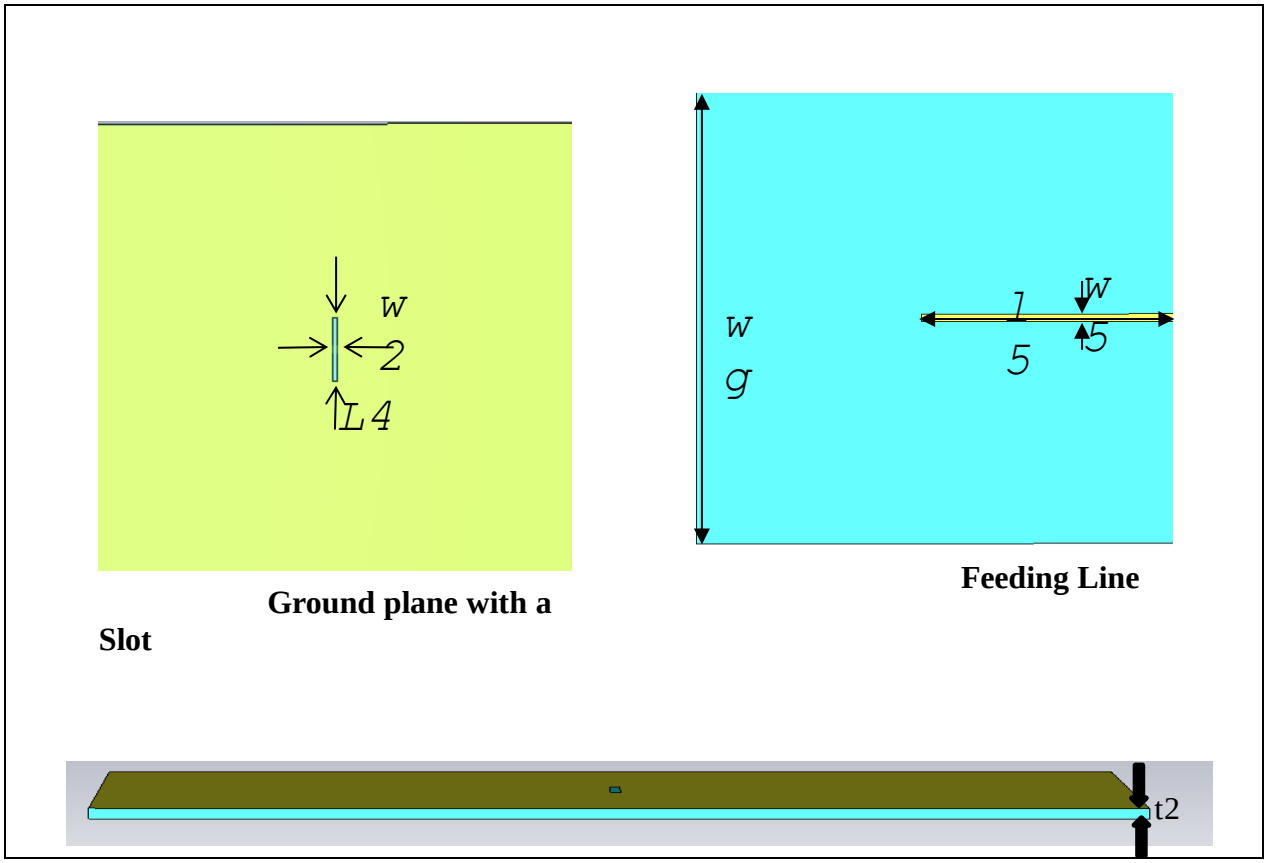


**Ground plane with a Slot**

**Feeding Line**

Figure 20:Basic antenna structure without metasurface

The antenna without metasurfaces uses basic and standard materials to support simple single-mode radiation. The table 8 outlines the materials used in its construction:

Table 8:the materials used in the antenna

| **Component** | **Material** |
|---|---|
| **Ground Plane** | Copper |
| **Substrate (Bottom)** | Taconic (εr = 2.65) |
| **Feeding Microstrip** | Copper |

This version of the antenna employs carefully chosen dimensions to support basic radiation

without modal enhancement. The table 9 presents the key physical dimensions used in the design:

Table 9:Dimensional parameters of the wide beam antenna without metasurface

| Parameter | Value (mm) | Description |
|---|---|---|
| **W2** | 1 | Width of the slot in ground plane |
| **L4** | 14 | Length of the slot in ground plane |
| **W5** | 1.7 | Width of microstrip feed line |
| **L5** | 53 | Length of microstrip feed line |
| **t2** | 0.5 | Thickness of bottom substrate |
| **Wg** | 100 | width of the ground plane |

- **$S_{11}$ Parameter**

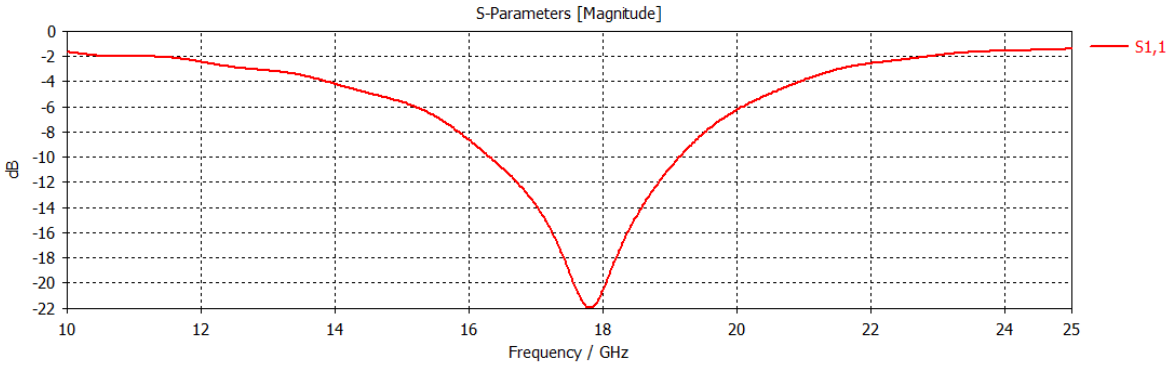


Figure 21:$S_{11}$ performance of basic antenna

The reflexion coefficient is calculated and plotted in Figure 21. The basic antenna structure, without metasurfaces, demonstrates a single weak resonance around **17 GHz**, where the $S_{11}$ reaches a minimum of approximately **−22 dB**. However, outside this point, the reflection coefficient remains relatively high, indicating poor matching and low radiation efficiency throughout most of the band. The lack of multiple resonant modes and the absence of any wideband behavior highlight the fundamental limitations of the slot-only configuration.

- **Radiation Pattern**

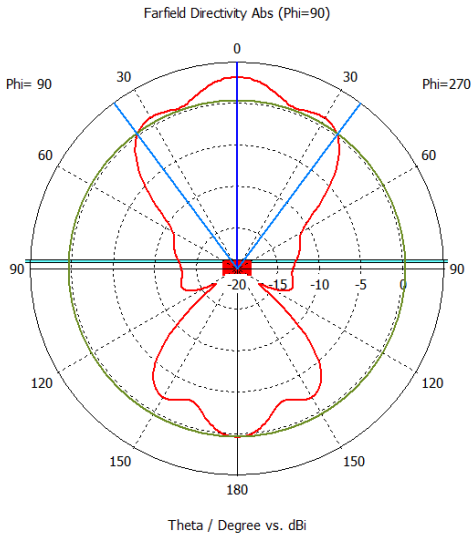


Figure 22:Radiation pattern at resonance frequency of 17.86 GHz

The radiation performance of the antenna without metasurfaces was analyzed at its resonance frequency of 17.86 GHz, as illustrated in Figure 22. At this frequency, the antenna achieves a peak gain of 3.32 dBi, with the main lobe directed at 0° and a 3 dB beamwidth of 66.8°. Although the radiation is moderately directional, the overall beam control remains limited. The broader pattern and moderate gain reflect the structural simplicity of the design.

- **Gain Performance**

The gain response of the antenna without metasurfaces exhibits moderate variation across the 10–25 GHz frequency range. A peak gain of approximately **7.5 dBi** is achieved near **20 GHz**, with other notable local maxima around **17 GHz** and **22 GHz**. However, the gain response is not uniformly stable, showing noticeable fluctuations rather than smooth, consistent performance. At the expected resonance frequency near **17.86 GHz**, the gain is approximately **6.9 dBi**, indicating reasonable but not optimal efficiency. The irregular gain profile and absence of broadband stability suggest that the basic antenna structure has inherent limitations. These observations underscore the potential benefits of integrating metasurfaces to enhance gain uniformity, bandwidth, and overall radiation efficiency.

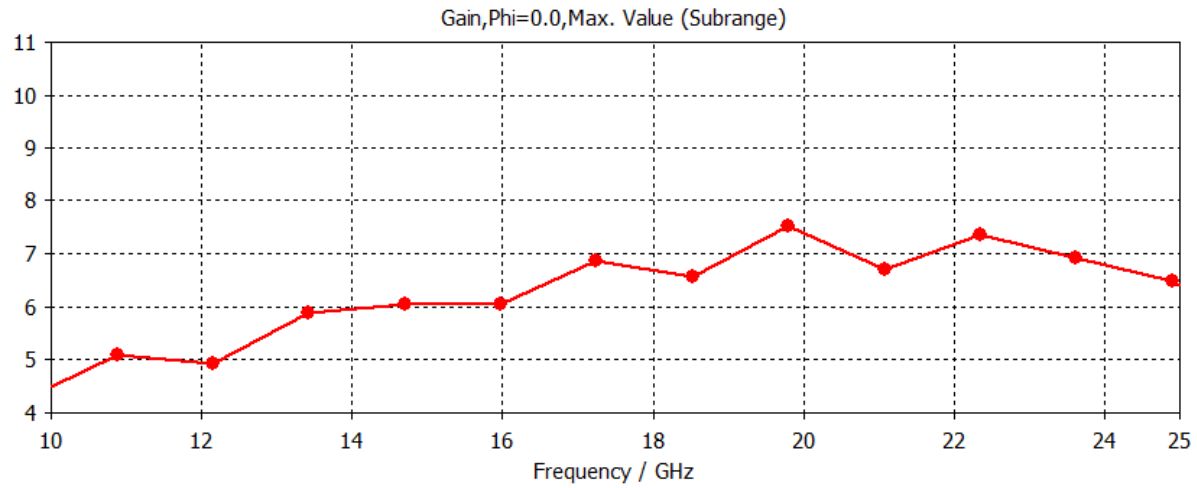


Figure 23:Gain performance of the basic antenna

- **Performance Limitations Without MTS**

The antenna in its basic form, without metasurface integration, demonstrates several performance limitations. It exhibits poor impedance matching across a wide frequency range, with a single weak resonance at 17.86 GHz and an $S_{11}$ minimum of only −16 dB. Radiation patterns lack stability, and gain performance is inconsistent, peaking irregularly outside the intended operating band. These issues highlight the restricted bandwidth, low modal control, and insufficient efficiency of the slot-only configuration, clearly justifying the need for metasurface enhancement.

## II.3.2 Metasurface (MTS) structure Analysis

- **MTS Design**

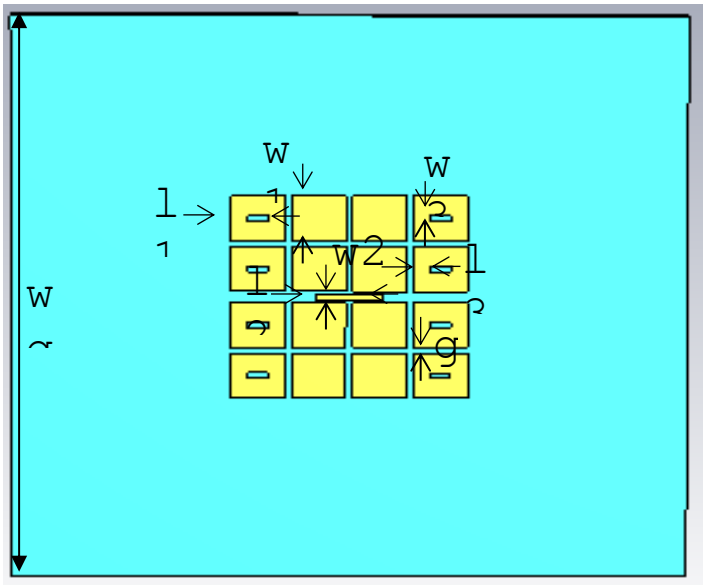


Figure 5:top view of the antenna with MTS

The enhanced antenna design incorporates a non-periodic metasurface (MTS) layer to improve radiation characteristics through the complementary sources concept. This metasurface is implemented using an array of rectangular copper patches, carefully placed on the top dielectric substrate. Each patch is dimensioned to interact constructively with the fields radiated from the central slot, enabling optimized surface current distribution and wide-beam performance. A top view of the MTS layout showing the patch dimensions (w1) and gap spacing (g) is illustrated in Figure 24, and the specific values are detailed in Table 12(page49).

- **Characteristic Mode Analysis (CMA) of the proposed MTS**

To better understand the electromagnetic behavior of the second MTS design, Characteristic Mode Analysis (CMA) is carried out. This approach reveals the natural modes supported by the structure and highlights those most relevant to radiation. By examining the Modal Significance (MS) across the frequency range, we can identify the active modes and their impact on the antenna's performance.

- **Results of the Characteristic Mode Analysis**

The following results, see table 10, present the CMA performed at a specific frequency, highlighting the characteristic modes supported by the structure and their significance at that operating point.

Table 10:Characteristic Mode Analysis results for the second antenna design showing 10 modes with radiation patterns and current distributions

| Mode1 | Mode2 | Mode3 |
|---|---|---|
| 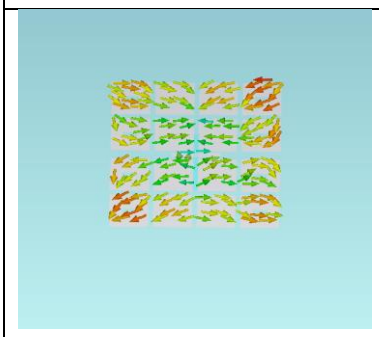 | 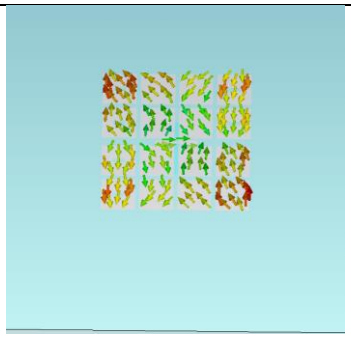 | 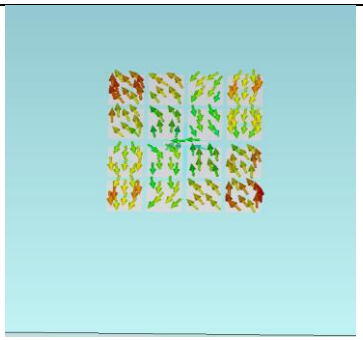 |
| 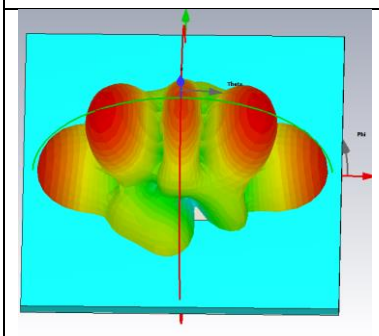 | 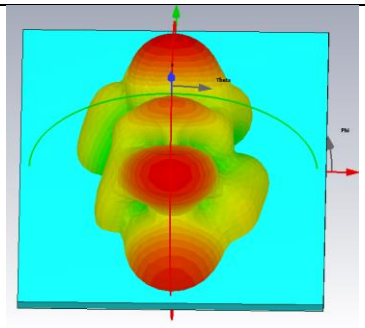 | 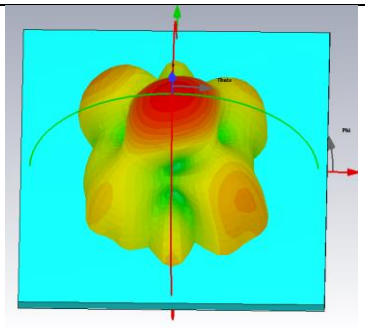 |
| **Mode4** | **Mode5** | **Mode6** |
| 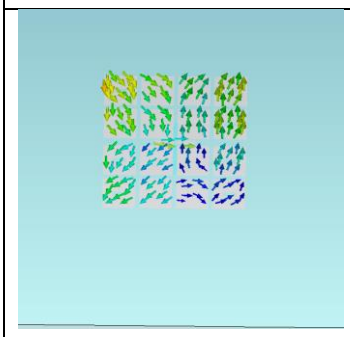 | 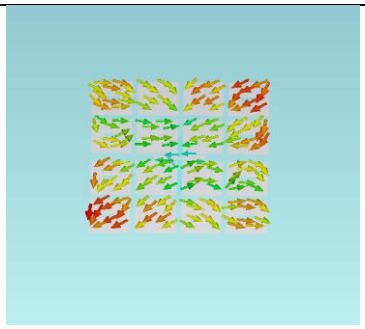 | 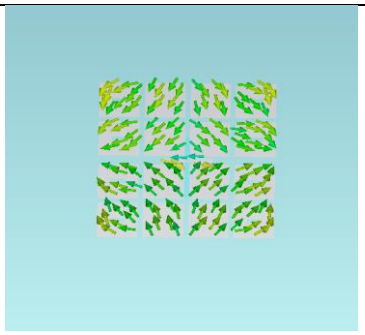 |
| 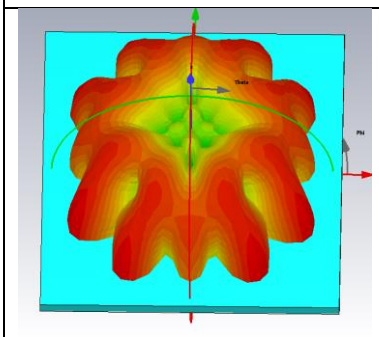 | 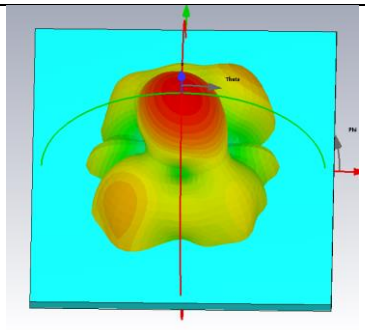 | 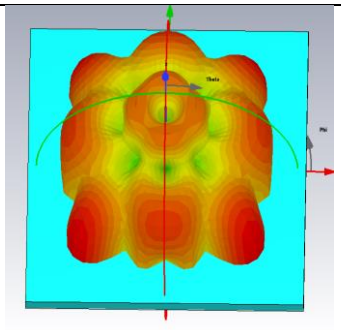 |

| Mode7 | Mode8 | Mode9 |
|---|---|---|
| 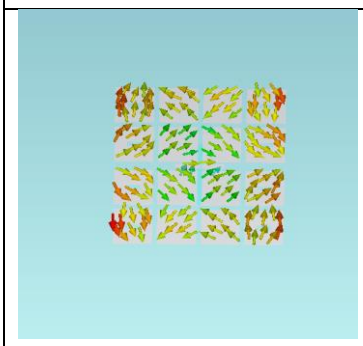 | 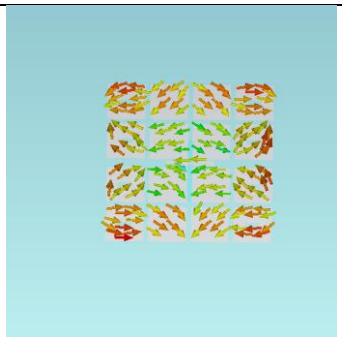 | 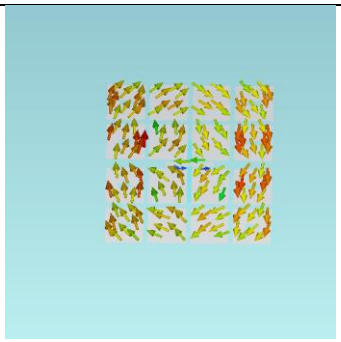 |
| 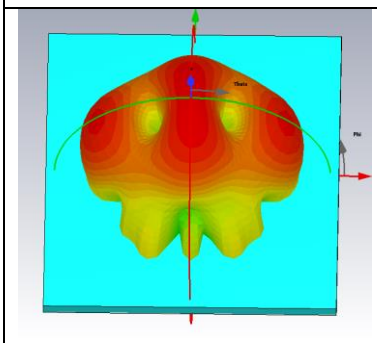 | 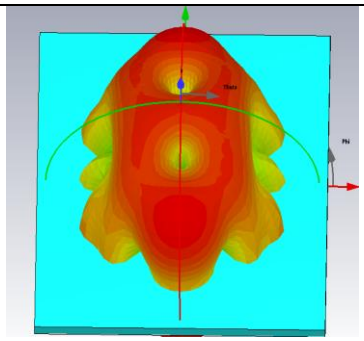 | 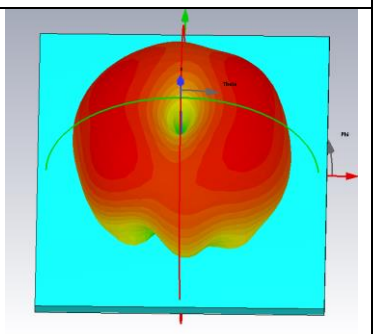 |

| Mode10 |
|---|
| 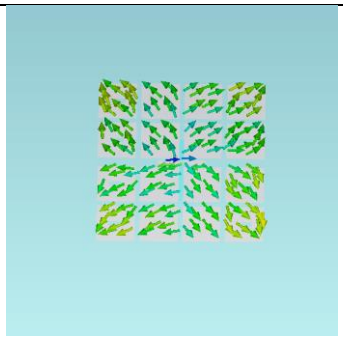 |
| 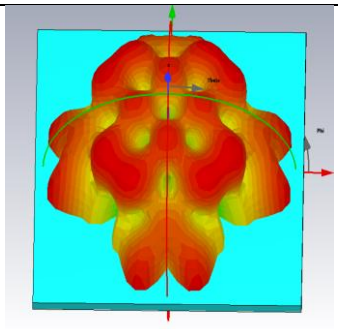 |

**Mode 1:**

- **Surface Current:** Magnitude of 14.4 dB(A/m), indicating moderate current excitation.

- **Farfield Radiation:** Directivity of 6.22 dBi with a relatively broad and less focused pattern. The pattern is symmetrical but lacks high directivity, suggesting limited efficiency.

**Mode 2:**

- **Surface Current:** Magnitude of 18.9 dB(A/m), indicating a stronger current distribution.
- **Farfield Radiation:** Directivity of 8.85 dBi with a multi-lobed pattern, showing moderate focus.
- The pattern shows some directionality, but the current magnitude suggests potential for better performance.

**Mode 3:**

- **Surface Current:** Highest magnitude at 23.3 dB(A/m), indicating excellent current excitation.
- **Farfield Radiation:** Directivity of 10.65 dBi with a well-defined, focused pattern.
- This mode shows strong potential for high radiation efficiency due to its focused pattern and high current.

**Mode 4:**

- **Surface Current:** Magnitude of 17.2 dB(A/m), showing decent current distribution.
- **Farfield Radiation:** Directivity of 4.78 dBi with a broad, less directional pattern.
- The low directivity suggests it may not be optimal for focused applications.

**Mode 5:**

- **Surface Current:** Magnitude of 20.0 dB(A/m), indicating strong current excitation.
- **Farfield Radiation:** Highest directivity at 11.02 dBi with a highly focused pattern.
- This mode stands out for its excellent directional performance and robust current flow.

**Mode 6:**

- **Surface Current:** Magnitude of 15.9 dB(A/m), showing moderate current distribution.

- **Farfield Radiation:** Directivity of 6.16 dBi with a broad pattern.
- Similar to Mode 1, it lacks strong directionality and efficiency.

**Mode 7:**

- **Surface Current:** Magnitude of 16.1 dB(A/m), indicating moderate current.
- **Farfield Radiation:** Directivity of 7.42 dBi with a multi-lobed pattern.
- The pattern shows some focus, but the current magnitude is relatively low.

**Mode 8:**

- **Surface Current:** Magnitude of 17.2 dB(A/m), showing decent current distribution.
- **Farfield Radiation:** Directivity of 6.37 dBi with a broad pattern.
- Similar to Mode 4, it has limited directional performance.

**Mode 9:**

- **Surface Current:** Magnitude of 17.2 dB(A/m), showing moderate current.
- **Farfield Radiation:** Directivity of 6.22 dBi with a broad, less focused pattern.
- Performance is comparable to Mode 1, with no significant advantage.

**Mode 10:**

- **Surface Current:** Magnitude of 15.9 dB(A/m), indicating moderate current distribution.
- **Farfield Radiation:** Directivity of 4.68 dBi with a very broad pattern.
- This mode shows the lowest directivity, suggesting poor directional efficiency.

The best mode should balance high directivity (from far field radiation) with strong surface current magnitude, as these factors indicate efficient radiation and energy transfer. Mode 5 excels with the highest directivity (11.02 dBi) and a significant surface current (20.0 dB(A/m)), making it the top performer for applications requiring focused radiation and robust current excitation. Mode 3 is a close second with a directivity of 10.65 dBi and the highest current magnitude (23.3 dB(A/m)), suggesting excellent energy transfer but slightly less directional focus than Mode 5. Mode 2 (8.85 dBi, 18.9 dB(A/m)) and Mode 7 (7.42 dBi, 16.1 dB(A/m))

show moderate performance, with Mode 2 having a better combination of directivity and current. Modes with lower directivity (e.g., Mode 4, Mode 10) and moderate current magnitudes are less optimal due to their broad patterns and reduced efficiency. Best Mode: Mode 5 is the best overall due to its superior directivity and strong current distribution, followed by Mode 3 for its exceptional current magnitude.

- **Modal Significance (MS) Results**

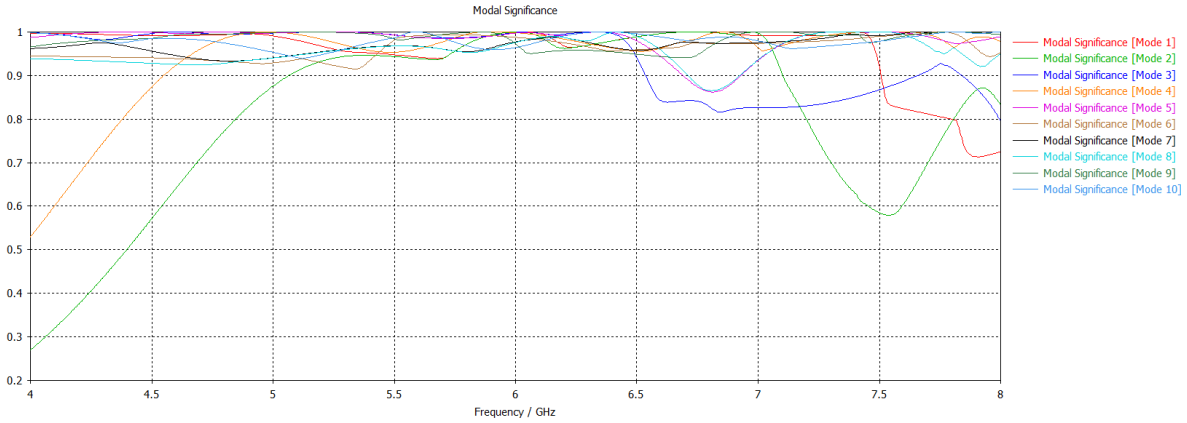


Figure 25:Modal Significance curves for different modes

The MS plotted in Figure 25 shows the significance of each mode across the frequency range (4-8 GHz).

- **Mode 1** and **Mode 4** maintain high and stable MS values (>0.8) from 5.5 GHz to 6.5 GHz, indicating strong modal activity and a broad operational bandwidth around 6 GHz.
- **Mode 2** peaks around 6 GHz but drops significantly beyond 6.5 GHz, suggesting a narrower bandwidth of significance.
- **Mode 5** shows a stable MS profile around 6 GHz, aligning with its strong performance in farfield and current metrics.
- Modes like **Mode 7**, **Mode 10**, and others exhibit lower and less consistent MS values, indicating weaker modal resonance across the frequency range.

The Mode 1 and Mode 4 curves are the best due to their high and stable MS values over a wider frequency range (5.5-6.5 GHz), making them suitable for broadband applications. Mode 5 also has a notable MS profile around 6 GHz, reinforcing its overall performance when combined with its farfield and current results.

These results confirm that Mode 5 emerges as the best overall mode, supported by its superior

farfield radiation (11.02 dBi) and significant surface current (20.0 dB(A/m)), making it ideal for focused radiation applications. Mode 3 stands out as a strong alternative, boasting the highest current magnitude (23.3 dB(A/m)) and a robust directivity (10.65 dBi), ensuring excellent energy transfer. Additionally, for broadband performance, Mode 1 and Mode 4 provide the best MS curves, offering stability across the 5.5-6.5 GHz range, which solidifies their suitability for wider frequency applications.

### II.3.3 Study of Antenna with Metasurface (MTS)

- **Final Design Architecture:**

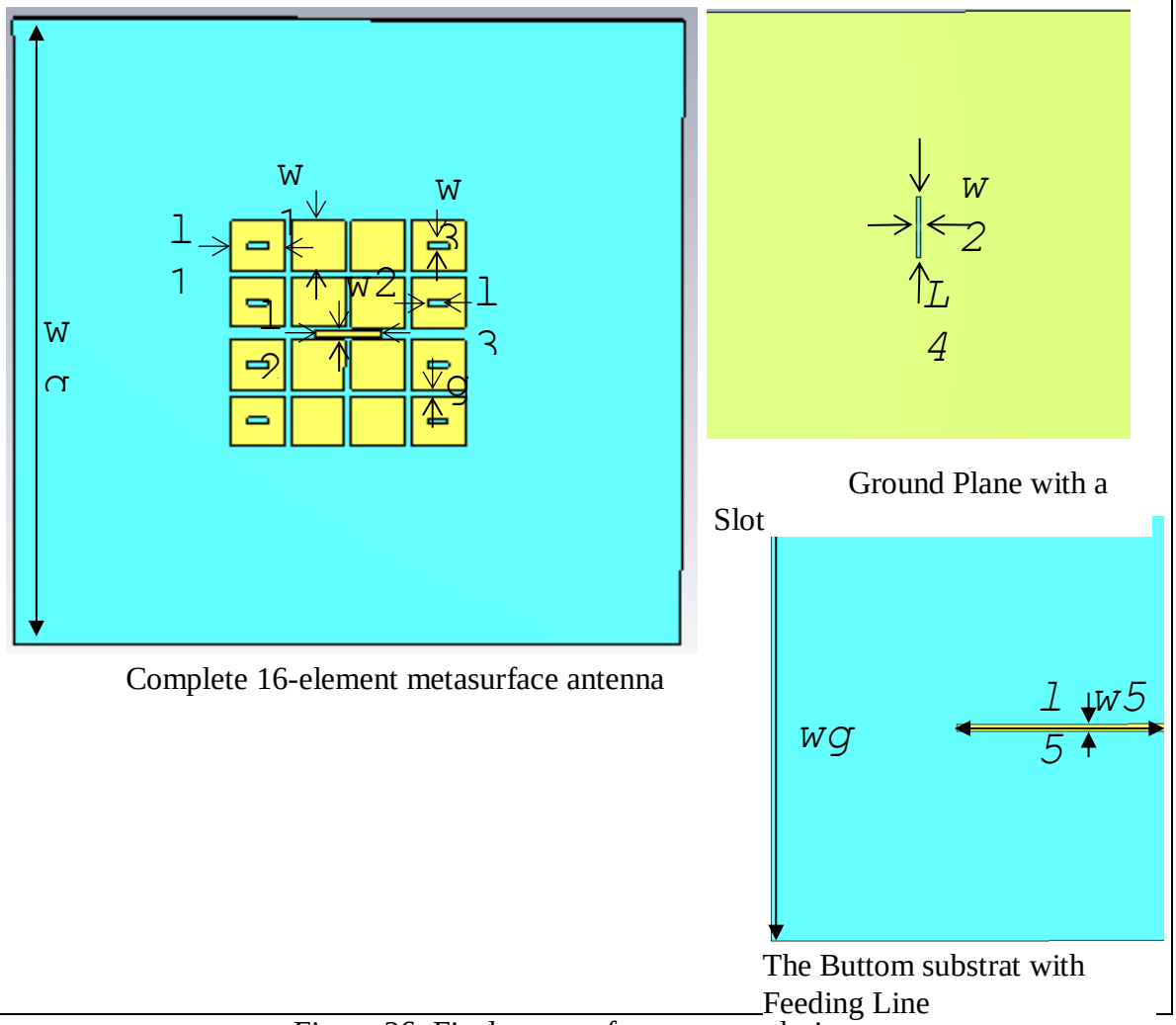


Figure 26: Final metasurface antenna design

The final antenna integrates a sophisticated 16-element metasurface with rectangular patches of identical dimensions, optimized gap spacing, and strategic slot adjustments on lateral patches

for modal behavior control. The central metal strip enhances coupling efficiency between the feeding slot and metasurface elements.

The three-layer architecture combines the metasurface layer (εr=3.5), ground plane with central feeding slot, and microstrip substrate (εr=2.65), as shown in Figure 26. This configuration enables precise implementation of the complementary sources concept through controlled excitation of quasi-$TM_{01}$ and quasi-$TM_{03}$ modes.

The ultra-low profile design ($0.08\lambda_0$) maintains compactness while achieving unprecedented 220° beam width through optimized modal superposition. The rectangular slots on side patches provide fine-tuning capability for Mode 8 resonance frequency alignment.

The antenna with metasurfaces is built using carefully selected materials to support multimode resonance and enhanced radiation performance. The table 11 summarize the materials used in its construction:

Table 11:Specification of materials for the improved antenna by metasurface

| **Component** | **Material** |
|---|---|
| **Top Substrate** | Taconic (εr = 3.5) |
| **Metasurface Patches** | Copper |
| **Ground Plane** | Copper |
| **Bottom Substrate** | Taconic (εr = 2.65) |
| **Feeding Microstrip** | Copper |

The table 12 presents the key physical dimensions used in the design.

Table 12:Dimensional parameters of the antenna with metasurface

| **w1** | **w2** | **w3** | **w4** | **w5** | **t1** | **t2** |
|---|---|---|---|---|---|---|
| 8 | 1 | 1 | 0.8 | 1.7 | 4 | 0.5 |
| **l1** | **l2** | **l3** | **l4** | **l5** | **wg** | **g** |
| 9.9 | 10 | 3 | 14 | 53 | 100 | 1 |

- **$S_{11}$ Parameter**

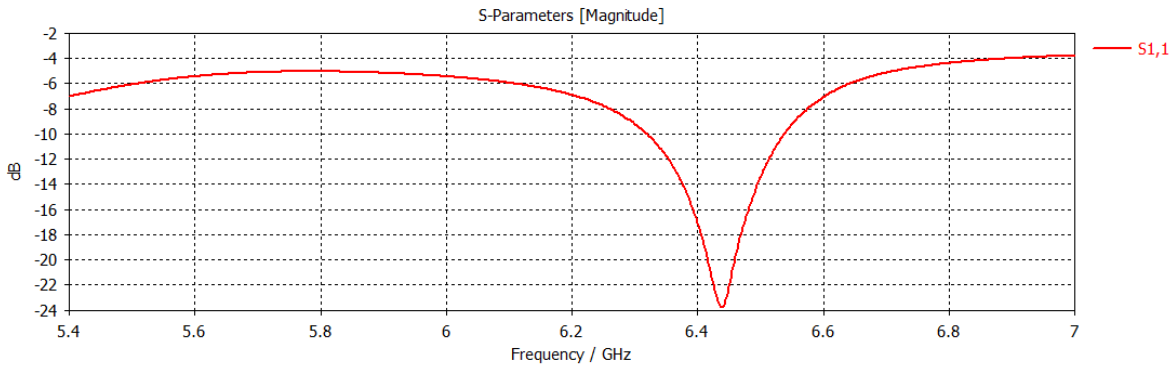


Figure 27:$S_{11}$ response of the final design

The metasurface transforms impedance characteristics with deep resonance at 6.4 GHz reaching -25 dB. The simulated bandwidth of 5.5% (6.3-6.47 GHz) perfectly covers Sub-6GHz applications. It can be concluded that the MTS leads to a high miniaturization by shifting the frequency from 17 GHz to 6 GHz.

This represents a dramatic improvement from the basic antenna's poor matching, validating the complementary sources concept and modal optimization strategy.

- **Gain Performance Analysis**

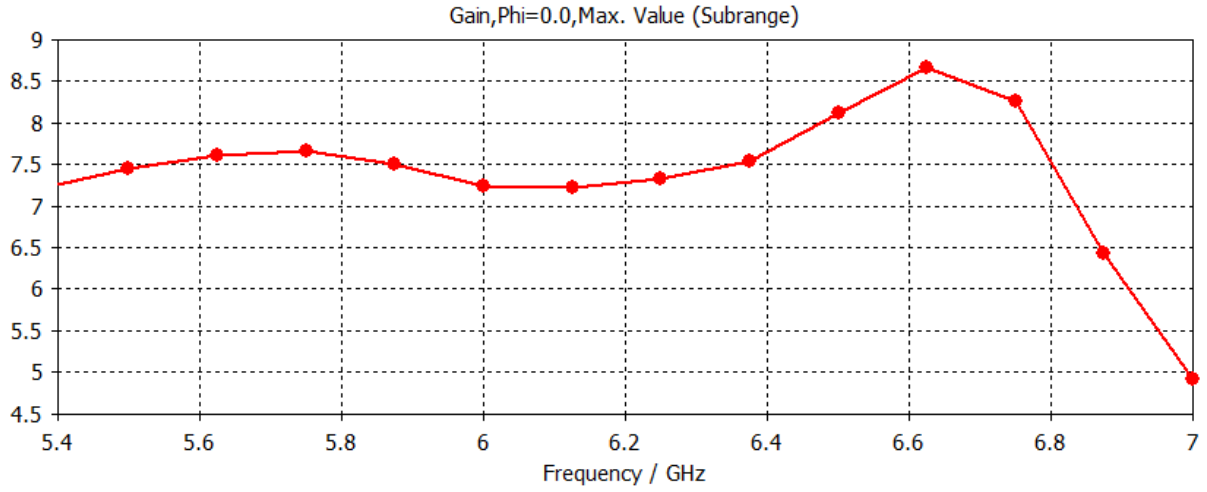


Figure 28:Stable gain performance

In the 5.4–7 GHz frequency band, the antenna with metasurfaces exhibits outstanding gain behavior, starting at approximately **6 dBi** and reaching a **peak of almost 9 dBi around 6.6**

**GHz**. The gain remains stable across the band, with a gradual and controlled roll-off beyond the resonance point. This consistent high-gain response demonstrates the effectiveness of the metasurface in supporting efficient radiation and makes the antenna well-suited for WLAN applications that require uniform and reliable coverage.

- **Radiation Pattern**

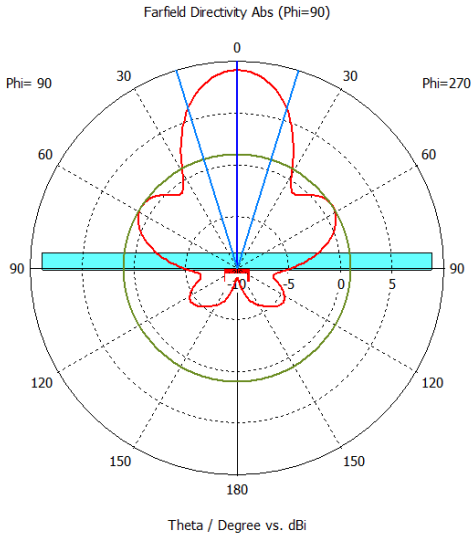


Figure 29: radiation pattern at 6.53 GHz

Figure 29 highlights the radiation characteristics of the antenna, focusing on the angular coverage, beam symmetry, and pattern stability achieved through metasurface integration. These results are illustrated in the far-field radiation pattern shown in the accompanying polar plot. At the frequency of **6.53 GHz**, the antenna exhibits excellent far-field radiation characteristics, achieving a **peak gain of 9 dBi**. The radiation pattern is highly directive with a **broadside orientation (0°)** and features **strong side lobe suppression of −8.1 dB**, indicating a well-focused main beam and reduced interference from secondary lobes. This performance reflects the precise control introduced by the complementary sources concept, which enables modal shaping and optimized field distribution.

The radiation pattern is not only highly directional but also symmetric and stable, confirming the antenna's capability to maintain high-quality performance at its resonant point. The balance between gain, directionality, and sidelobe control demonstrates the effectiveness of the metasurface design and validates the robustness of the structural optimization strategy at this frequency.

- **Performance Limitations With MTS**

While the antenna with metasurfaces exhibits significant improvements in bandwidth, gain, and radiation control, certain limitations remain. The gain, although stable and high across the main operating band, shows a gradual decline beyond the resonance frequency, limiting performance at higher frequencies. Additionally, the beamwidth narrows at specific bands, which may reduce coverage uniformity in ultra-wideband scenarios. Fabrication complexity and sensitivity to alignment of metasurface elements may also affect repeatability and practical implementation. Despite these minor constraints, the metasurface-enhanced design still offers substantial advantages over the basic configuration.

## II.3.4 Comparative Analysis: With vs Without Metasurface

In this analysis, we will compare the performance of the antenna with and without a metasurface (MTS) by examining S11, radiation patterns, and gain performance to determine the impact of MTS integration.

- **Comparison of $S_{11}$**

The S11 performance shows distinct differences, with the with metasurface configuration offering a deeper minimum S11 value and a more defined bandwidth, indicating better impedance matching:

Table 13: Comparative performance analysis $S_{11}$

| **Aspect** | **Without Metasurface** | **With Metasurface** |
|---|---|---|
| **Frequency Range** | 4–20 GHz | 5–7 GHz |
| **Minimum $S_{11}$ Value** | Approximately −14 dB | Approximately −26 dB |
| **Bandwidth of $S_{11} < -10$ dB** | Broad but less defined | Well-defined around 5.8–6.2 GHz |
| **Resonance Peaks** | Multiple shallow peaks | Single deep resonance |

- **Comparison of Radiation Pattern**

Table 14:Comparative performance analysis of Radiation pattern

| Aspect | Without Metasurface | With Metasurface |
|---|---|---|
| **Frequency** | 17.8597 GHz | 6.5279 GHz |
| **Main Lobe Magnitude** | 6.9 dB | 9.12 dB |
| **Main Lobe Direction** | 0.0° | 0.0° |
| **Angular Width (3 dB)** | 66.4° | 34.4° |
| **Side Lobe Level (SLL)** | −2.6 dB | −8.1 dB |
| **Pattern Shape** | Broader with higher sidelobes | More focused with lower sidelobes |

The radiation pattern comparison highlights that the with metasurface design provides a narrower angular width and significantly lower side lobe levels, indicating improved directivity and reduced interference compared to the broader pattern of the without metasurface design.

## II.4 Conclusion

This chapter compared two metasurface antenna designs: one for broadband performance via multimode resonance, and another for wide-beam radiation using the complementary sources concept.

Both were evaluated with and without metasurfaces using return loss, gain, radiation patterns, and CMA.

Metasurfaces were shown to enhance performance through multiple resonances, better matching, and stable patterns.

CMA highlighted the importance of selecting high-significance modes for bandwidth and radiation control.

The combination of MTS and CMA produced compact, efficient antennas fit for modern wireless needs.

These results confirm the value of merging surface engineering with modal analysis

# General Conclusion

This work has explored, in a comprehensive and detailed manner, the complementary roles of **Metasurfaces (MTS)** and **Characteristic Mode Analysis (CMA)** in the design and optimization of modern antenna systems. These two technologies, although distinct in nature, converge in their capacity to advance electromagnetic design and improve antenna performance significantly.

**Metasurfaces**, as two-dimensional engineered surfaces composed of subwavelength elements, have demonstrated remarkable abilities in manipulating electromagnetic wavefronts. Their unique capacity to control phase, amplitude, and polarization makes them highly effective for achieving **wideband operation**, **beam shaping**, and **beam steering**—functions that are increasingly demanded in high-frequency and compact wireless systems. The integration of metasurfaces allows designers to overcome many limitations of conventional antenna structures, especially in terms of profile reduction, multi-functionality, and enhanced radiation efficiency.

On the other hand, **Characteristic Mode Analysis (CMA)** provides a powerful theoretical and numerical framework for understanding the intrinsic resonant behavior of conducting structures. By decomposing complex current distributions into a set of orthogonal modes with physical significance, CMA enables engineers to isolate and manipulate the modal contributions responsible for radiation. This understanding leads to informed decisions about **optimal feed placement**, **modal excitation**, and **bandwidth enhancement**, facilitating a more systematic and predictive approach to antenna design.

The synergy between MTS and CMA has proven to be particularly impactful. While metasurfaces offer new degrees of freedom for electromagnetic manipulation, CMA ensures that these structures are optimally exploited by revealing the most effective modes to activate or suppress. In this thesis, two antenna configurations were designed and analyzed—one aiming for **broadband performance through multimode resonance**, and the other focused on **wide-beam radiation using the complementary sources concept**. Both designs were studied with and without metasurfaces, using detailed simulations supported by CMA. The results clearly demonstrated that the **integration of MTS and CMA leads to antennas that are more compact, efficient, and versatile**, while also achieving superior characteristics in

terms of return loss, gain, radiation stability, and directivity.

Moreover, this work confirms that the combination of surface engineering and modal analysis is not only theoretically sound but also practically powerful, especially for current and future applications in **5G**, **WLAN**, **IoT**, and beyond. The enhanced control over antenna behavior, achieved through these techniques, paves the way for next-generation wireless systems that are **reconfigurable**, **miniaturized**, and **performance-optimized**.

Looking forward, several promising research directions emerge. These include the use of **AI and machine learning** to automate and optimize metasurface design based on modal characteristics; the development of **reconfigurable or tunable metasurfaces** using advanced materials like graphene or liquid crystals; and the application of these principles to **wearable**, **implantable**, or **aerospace platforms** where size, weight, and power consumption are critical constraints.

In conclusion, the fusion of Metasurface technology and Characteristic Mode Analysis represents a **transformative approach** in modern antenna engineering. Together, they offer a robust and scalable pathway for designing high-performance electromagnetic systems capable of meeting the evolving challenges of wireless communication in the 21st century.

## References


[1] S. S. Bukhari, J. Vardaxoglou and W. Whittow, “A Metasurfaces Review: Definitions and Applications,” *Applied Sciences,* vol. 9, no. 13, p. 2727, 2019.

[2] Christopher L. Holloway, “An Overview of the Theory and Applications of Metasurfaces: The Two-Dimensional Equivalents of Metamaterials,” *IEEE Antennas and Propagation Magazine,* vol. 54, no. 2, p. 10–35, 2012.

[3] Nanfang Yu, “Light Propagation with Phase Discontinuities: Generalized Laws of Reflection and Refraction,” *Science,* vol. 334, no. 6054, p. 333–337, 2011.

[4] Grbic, “Metamaterial Huygens' Surfaces: Tailoring Wave Fronts with Reflectionless Sheets,” *Physical Review Letters,* vol. 110, no. 19, p. 197401, 2013.

[5] Ding, “A review of gap-surface plasmon metasurfaces: fundamentals and applications,” *Nanophotonics,* vol. 7, no. 6, pp. 1129--1156, 2018.

[6] N. Meinzer, “Plasmonic Meta-atoms and Metasurfaces,” *Nature Photonics,* vol. 8, no. 12, p. 889–898, 2014.

[7] P. Genevet, “Recent Advances in Planar Optics: From Plasmonic to Dielectric Metasurfaces,” *Optica,* vol. 4, no. 1, p. 139–152, 2017.

[8] F. Ding, “Gradient Metasurfaces: A Review of Fundamentals and Applications,” *Reports on Progress in Physics,* vol. 82, no. 2, p. 026401, 2018.

[9] S. Chen, “Phase Manipulation of Electromagnetic Waves with Metasurfaces and Its Applications in Nanophotonics,” *Advanced Optical Materials,* vol. 6, no. 13, p. 1800104, 2018.

[10] S. Sun, “Electromagnetic Metasurfaces: Physics and Applications,” *Advances in Optics and Photonics,* vol. 11, no. 2, pp. 380-479, 2019.

[11] W. T. Chen, “Flat Optics with Dispersion-Engineered Metasurfaces,” *Nature Reviews Materials,* vol. 5, no. 8, pp. 604-620, 2019.

[12] Y. Chen, “Programmable metasurface-based coding for intelligent electromagnetic manipulation,” *eScience,* vol. 5, no. 2, p. 227–234, 2024.

[13] R. Wu, “Intelligent reflecting surface enhanced wireless network via joint active and passive beamforming,” *IEEE Transactions on Wireless Communications,* vol. 18, no. 11, pp. 5394-5409, 2021.

[14] M. D. Renzo, “Smart radio environments empowered by reconfigurable intelligent surfaces: How it works, state of research, and the road ahead,” *IEEE Journal on Selected Areas in Communications,* vol. 38, no. 11, p. 2450–2525, 2020.

[15] W. a. J. Lee, “Single-layer phase gradient mmWave metasurface for incident angle independent focusing,” *Scientific Reports,* vol. 11, p. 12671, 2021.

[16] G. Minatti, “Spiral leaky-wave antennas based on modulated surface impedance,” *IEEE Transactions on Antennas and Propagation,* vol. 59, no. 12, p. 4436–4444, 2011.

[17] A. Epstein, “Cavity-excited Huygens' metasurface antennas for near-unity aperture illumination efficiency from arbitrarily large apertures,” *Nature Communications,* vol. 7, p. 10360, 2016.

[18] F. Aieta, "Aberration-Free Ultrathin Flat Lenses and Axicons at Telecom Wavelengths Based on Plasmonic Metasurfaces," *Nano Letters,* vol. 12, no. 9, p. 4932–4936, 2012.
[19] X. Ni, "Metasurface Holograms for Visible Light," *Nature Communications,* vol. 4, p. 2807, 2013.
[20] R. J. Garbacz, "Modal expansions for resonance scattering phenomena," *Proceedings of the IEEE,* vol. 53, no. 8, pp. 856-864, 1965.
[21] R. F. Harrington, "Theory of characteristic modes for conducting bodies," *IEEE Transactions on Antennas and Propagation,* vol. 19, no. 5, pp. 622-628, 1971.
[22] M. Capek, "Validating the Characteristic Modes Solvers," *IEEE Transactions on Antennas and Propagation,* vol. 65, no. 8, pp. 4134-4145, 2017.
[23] M. Capek, "Original structure to be decomposed into characteristic modes discretized using Delaunay triangulation," *Wikimedia Commons,* 24 7 2017.
[24] M. Cabedo-Fabres, "The Theory of Characteristic Modes Revisited: A Contribution to the Design of Antennas for Modern Applications," *IEEE Antennas and Propagation Magazine,* vol. 49, no. 5, p. 52–68, 2007.
[25] M. Capek, "A Method for the Evaluation of Radiation Q Based on Modal Approach," *IEEE Transactions on Antennas and Propagation,* vol. 60, no. 10, p. 4556–4567, 2012.
[26] Bernhard, "Broadband Equivalent Circuit Models for Antenna Impedances and Fields Using Characteristic Modes," *IEEE Transactions on Antennas and Propagation,* vol. 61, no. 8, p. 3985–3994, 2013.
[27] Adams, "Computing and Visualizing the Input Parameters of Arbitrary Planar Antennas via Eigenfunctions," *IEEE Transactions on Antennas and Propagation,* vol. 64, no. 7, p. 2707–2718, 2016.
[28] Harrington, Field Computation by Moment Methods, Wiley-IEEE Press, 1993, p. 240.
[29] Zhang, "Data-driven multi-mode far-field beam manipulation using metasurface antenna arrays," *eScience,* vol. 5, no. 2, p. 235–243, 2024.
[30] Dong, "Design of a twelve-port MIMO antenna system for multi-mode 4G/5G smartphone applications based on characteristic mode analysis," *IEEE Access,* vol. 8, pp. 90751--90759, 2020.
[31] E. Safin, "Manipulation of Characteristic Wave Modes by Impedance Loading," *IEEE Transactions on Antennas and Propagation,* vol. 63, no. 4, pp. 1756-1764, 2015.
[32] Minatti, "Spiral leaky-wave antennas based on modulated surface impedance," *IEEE Transactions on Antennas and Propagation,* vol. 59, no. 12, pp. 4436-4444, 2011.
[33] Shariff, "Characteristic Mode Analysis Based Highly Flexible Antenna For Millimeter Wave Wireless Applications," *Journal of Infrared, Millimeter, and Terahertz Waves,* vol. 45, pp. 1--26, 2024.